Deep-Sea Research II 55 (2008) 1988–2006

Contents lists available at ScienceDirect

Deep-Sea Research II

journal homepage: www.elsevier.com/locate/dsr2

Seasonal and interannual variability in temperature, chlorophyll and macronutrients in northern Marguerite Bay, Antarctica

Andrew Clarke [a,*], Michael P. Meredith [a], Margaret I. Wallace [a], Mark A. Brandon [b], David N. Thomas [c]

[a] British Antarctic Survey, NERC, High Cross, Madingley Road, Cambridge CB3 0ET, UK
[b] Department of Earth Sciences, Open University, Walton Hall, Milton Keynes MK7 6AA, UK
[c] School of Ocean Sciences, University of Wales Bangor, Menai Bridge, Anglesey LL59 5AB, UK

ARTICLE INFO

Article history:
Accepted 22 April 2008
Available online 6 August 2008

Keywords:
Seasonality
Ice
Oceanography
Mixed layer
Irradiance
Flux

ABSTRACT

We report data from the first 8 years of oceanographic monitoring in Ryder Bay, northern Marguerite Bay, Antarctica. These data form the oceanographic component of the *Rothera Oceanographic and Biological Time-Series* (RaTS) project. When weather and ice permit, the RaTS station is occupied every 5 days in summer and weekly in winter. Observations comprise a conductivity–temperature–depth (CTD) cast to 500 m and a water sample from 15 m, this being the depth of the chlorophyll maximum in most years. The water samples provide data on total chlorophyll (size-fractionated at 20, 5, 2 and 0.2 μm), macronutrients (N, P and Si) and dissolved organic carbon (DOC). The CTD profiles reveal strong seasonality in the topmost Antarctic Surface Water (AASW) driven by summer solar heating and winter cooling with brine rejection during ice formation. The depth of the winter mixed layer reaches a maximum in August, with annual maximum values ranging from ~30 to >140 m. Below the AASW is the relatively aseasonal Winter Water (WW), and the bottom of the profile indicates the presence of modified Upper Circumpolar Deep Water (UCDW). Summer chlorophyll typically exceeds 20 mg m^{-3}, with the peak in January. Vertical flux of phytodetritus is also predominantly in January. The summer bloom is dominated by large diatoms and colonial forms, whereas in winter most of the chlorophyll is in the nanophytoplankton (20–5 μm) fraction. Macronutrients show marked seasonality with N:P covariation close to Redfield (~15.3) and Si:N stoichiometry ~1.67. Summer DOC values show little seasonality and relatively high winter levels (>50 μM). Surface waters also exhibit a marked interannual variability, with ENSO as an important driver at subdecadal scales.

1. Introduction

The Southern Ocean is a highly seasonal environment. The high latitude dictates the marked annual variability in light climate, and this is exacerbated by the seasonal pattern of ice cover. As a result water-column primary production is markedly seasonal, and this seasonality propagates through the oceanic and benthic food-webs (Clarke, 1988). The strong seasonality makes it important to undertake year-round measurements, but logistic constraints limit most high-latitude oceanographic expeditions to the ice-free summer months. Satellite ocean-colour data can provide a seasonal summary of surface chlorophyll over a wide area (Korb and Whitehouse, 2004), and a representative seasonal picture can be constructed from measurements made at different times of the year (Whitehouse et al., 1996). Other aspects of the seasonal dynamics of the water column can be inferred from summer measurements (for example the input of glacial melt to surface waters: Dierssen et al., 2002). None of these approaches, however, can substitute for year-round data in generating a full seasonal picture. Usually such studies will involve work from shore-based research stations, and hence will typically concentrate on nearshore oceanography.

Unfortunately, few such studies have been undertaken in Antarctica. Single-year studies have established the broad features of the seasonal cycle at a small number of costal locations, including Mawson (Bunt, 1960), McMurdo Sound (Littlepage, 1965), Palmer Station, Anvers Island (Krebs, 1983) and King George Island (Kopczyńska, 1981). The longest series of year-sound measurements are, however, for Signy Island, South Orkney Islands (Clarke et al., 1988; Clarke and Leakey, 1996). These observations revealed important features that had not previously been recognised; in particular they demonstrated that although the summer phytoplankton bloom was dominated by diatoms, the nanoflagellate bloom was ecologically important in that it lasted longer, and in the depths of winter nanoflagellate chlorophyll levels exceeded those of diatoms.

* Corresponding author.
E-mail address: accl@bas.ac.uk (A. Clarke).

0967-0645/$ - see front matter © 2008 Elsevier Ltd. All rights reserved.
doi:10.1016/j.dsr2.2008.04.035

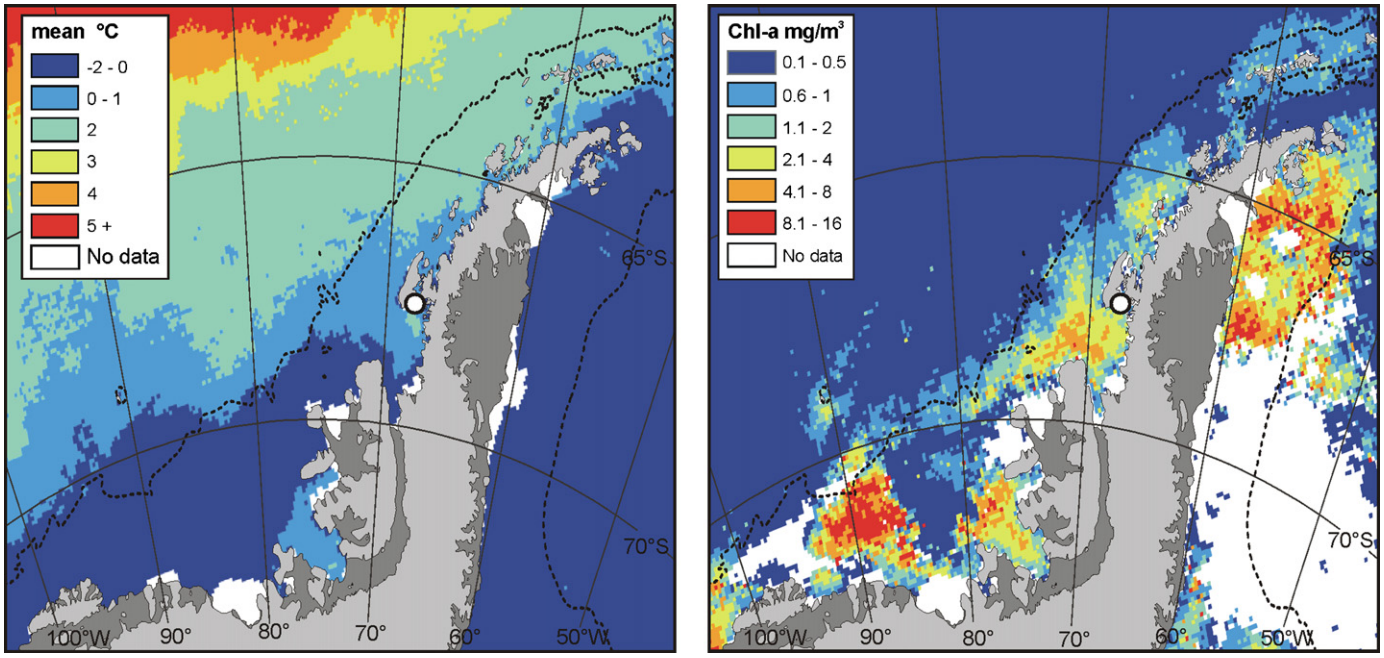

Fig. 1. The regional oceanographic context for the RaTS study, showing the location of Rothera research station in northern Marguerite Bay. Note that Ryder Bay is to the east of Adelaide Island, and the west of the Antarctic Peninsula. The edge of the continental shelf is marked by the 1000 m isobath (dashed line). (A) Sea-surface temperature from Aqua MODIS (1 km resolution). Data are for January, averaged over 2003–2006. (B) Chlorophyll, as estimated from SeaWiFS ocean colour. Data are for January, averaged over the period 1998–2006. Plots courtesy of Andrew Fleming, data courtesy of NERC Remote Sensing Data Analysis Service, Plymouth, UK.

The programme of year-round marine science at Signy ceased in 1994, and research moved to Rothera Point, Adelaide Island (Fig. 1). Here year-round oceanographic observations commenced in January 1997, with a series of regular oceanographic and biological observations that together constitute the *Rothera Oceanographic and Biological Time Series* (RaTS) programme, a component of the Long Term Monitoring and Survey core programme of the British Antarctic Survey (BAS). In this paper we present data from the first 8 years of the study. We concentrate on establishing the basic features of the annual (seasonal) cycle, but also report on some aspects of interannual variability.

1.1. The oceanographic context

The western Antarctic Peninsula (WAP) is unusual compared with most regions of Antarctica because of its proximity to the Antarctic Circumpolar Current (ACC) (Martinson et al., 2008). Other regions, such as the coasts of the Weddell and Ross Seas, are separated from the ACC by large regional gyres, whereas ACC waters lie immediately adjacent to the slope at the western edge of the western Antarctic Peninsula shelf. This proximity is significant, since it means that waters from the ACC can intrude directly onto the shelf in forms that are much less modified than elsewhere around the continent; glacially carved canyons are believed to be especially important in this context (Klinck, 1998; Hofmann and Klinck, 1998; Dinniman and Klinck, 2004). Of prime importance is Circumpolar Deep Water (CDW), the water mass that occupies the mid-levels of the ACC. This is usually divided into Upper (shallower) and Lower components (UCDW and LCDW, respectively), with UCDW being characterised by a maximum in potential temperature, relatively high nutrient contents, and a low oxygen content (Hofmann et al., 1996; Meredith et al., 2004). Incursions of UCDW are important in bringing heat and nutrients onto the continental shelf. Over the period 1993–2002, UCDW flooded large areas of the WAP continental shelf in most years, and this appears to be a reasonably consistent feature of shelf oceanography in this region (Ducklow et al., 2007).

The uppermost waters over the continental shelf are typically very much colder and fresher than UCDW, because of interaction with the atmosphere and cryosphere. Traditionally termed Antarctic Surface Waters (AASW), they typically cool and gain salt from sea-ice formation as summer moves into winter, then warm and freshen from winter to summer (Klinck, 1998). The AASW is thus thermally highly variable and solar heating can lead to strong stratification with relatively warm surface layers in summer; this seasonality is seen down to depths ~100 m (Meredith et al., 2004). The creation of a relatively warm and fresh surface layer during summer leads to isolation of the remnant of the cold winter mixed layer from the atmosphere. This results in a subsurface temperature minimum, traditionally referred to as Winter Water (WW: Mosby, 1936). WW temperatures are usually very close to the freezing point, but over the continental shelf of the WAP vertical mixing with the warmer waters above and below can lead to somewhat higher temperatures (Klinck, 1998; Smith and Klinck, 2002; Ducklow et al., 2007). The coastal oceanography along the western Antarctic Peninsula is thus dominated by the AASW at depths down to ~100 m, including WW at the lower levels.

A second important factor in the oceanography of the WAP area is its proximity to large quantities of glacial ice on land, and hence the influence of meltwater (Meredith et al., 2008). It is known that seasonal variability in the volume and spatial extent of glacial meltwater plays a critical role in oceanic ecosystem processes, particularly primary production (Dierssen et al., 2002), and also that water-column stability and a shallow mixed layer are essential to phytoplankton bloom development (Mitchell and Holm-Hansen, 1991). The addition of a thin lens of freshwater to the ocean surface will greatly increase its stability, thereby retaining phytoplankton within a favourable light environment by preventing mixing to depths where light is limiting. In the WAP

region, lower salinities are typically associated with a transition from a diatom-dominated system to one dominated by smaller cryptophytes (Moline et al., 2004).

1.2. Latitudinal and onshore/offshore gradients

Ryder Bay is situated in northern Marguerite Bay, towards the southern end of the Antarctic Peninsula. It lies to the east of Adelaide Island (Fig. 1) and is therefore slightly isolated from the open continental shelf. This position places the study at the southern end of environmental gradients extending along the western Antarctic Peninsula continental shelf, and at the nearshore end of across-shelf gradients. Specifically Marguerite Bay has lower summertime temperatures than the northern Antarctic Peninsula, and also experiences higher average chlorophyll concentrations (Fig. 1). In addition to these latitudinal trends, there are also strong gradients in many environmental factors across the continental shelf. In particular phytoplankton blooms tend to be higher nearshore, where surface waters also show a greater influence of glacial meltwater (Dierssen et al., 2002; Garibotti et al., 2003).

2. Materials and methods

2.1. Sampling station

The main RaTS sampling station is located in Ryder Bay (Fig. 2). It is situated ~4 km from shore, over a water depth of ~520 m. The station is reached by small boat during periods of open water and by snowmobile when winter fast-ice is safe to traverse. When the main RaTS station cannot be occupied, a secondary station is used. The aim is to obtain a water-column profile with a conductivity–temperature–depth (CTD) cast, and collect a single water sample from 15 m depth. If weather or ice prevents access to both the primary and secondary stations then a water bottle sample is taken from a third station close to the wharf, but because of the shallow depth no CTD cast is made. Station data are given in Table 1.

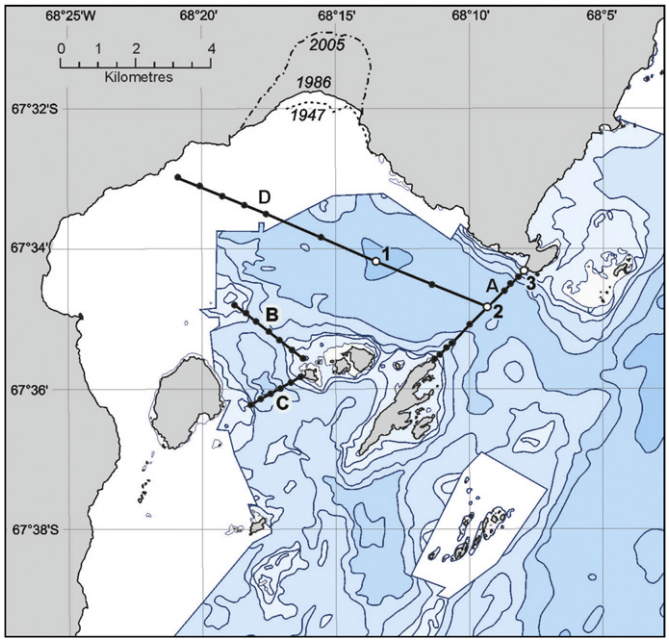

Fig. 2. Map of Ryder Bay, northern Marguerite Bay, showing main RaTS sampling stations. The main RaTS sampling stations are shown by open circles, and numbered 1–3 (data in Table 1). Also shown are four CTD transects occupied in January 2005 (A–D). The retreat of the Sheldon Glacier is shown by the position of the floating ice front in 1947 and 2005. Bathymetry contours are 100 m, and the main RaTS station (1) is positioned over >500 m water.

Table 1
Rothera Oceanographic and Biological Time Series (RaTS) stations, Ryder Bay, northern Marguerite Bay

Site	Latitude	Longitude	Depth (m)	Comment	*n*
1	67134.200′S	68113.500′W	520	Main RaTS station	344
2	67134.850′S	6819.340′W	~400	Secondary RaTS station	55
3	67134.330′S	6817.970′W	o 100	Biscoe Wharf	5

The final columns shows the total number of water sample events taken at each of the three sites over the period January 1997–December 2006.

2.2. Sampling protocol

A complete RaTS sample comprises a CTD cast to 500 m, followed by a water bottle sample from 15 m depth. These are given separate event numbers in the database, starting with event 001 on 1 January 1997; CTD profiles started in January 1998 with event 43. The aim is to occupy the RaTS station every 5 days in summer, and every 7 days in winter, except when weather, ice or logistic constraints intervene. The annual total of RaTS events ranges from 26 (2000) to 49 (1998), and the average number of events per month for the period 1997–2006) ranges from 6.7 in summer (January) to 1.9 in late winter (September). Two significant periods without data were June to December 2000 when persistent heavy but fractured sea-ice prevent access to any of the RaTS stations, and from 21 September 2001 when the laboratory was lost to fire, to 1 December 2001 when RaTS sampling restarted. In addition there was a small break at the start of the 2005/2006 season, when ice again prevented sampling for nearly 4 weeks.

From the start of the RaTS programme until January 2003 CTD casts were undertaken using a Chelsea Instruments Aquapak and fluorometer. Pressure certification limited these profiles to 200 m. From 2003 the CTD package has comprised a SeaBird 19+ CTD, together with a WetLabs in-line fluorometer and a LiCor PAR sensor. Data from all sensors are logged internally, with data collection being initiated by a seawater switch. The CTD package is lowered and recovered using a hand operated winch at a rate of 1 m s^{-1}. At the start of a cast, the CTD is lowered to 5 m and held at this depth for 15 min to allow the sensors to equilibrate. The unit is then brought to the surface before being lowered to full depth. Care is taken to ensure that the CTD is not shadowed by the boat as this would otherwise reduce the measured surface PAR values. Typically only data from the downcast are used.

The conductivity sensor is cross-calibrated annually with a SeaBird SBE 911+ CTD deployed in parallel with the Palmer-Long-Term Ecological Research (LTER) programme from the US research vessel *Laurence M. Gould*, and also with a similar instrument on the UK research vessel RRS *James Clark Ross*. These units are themselves calibrated using P-series IAPSO standard seawater.

Following the CTD cast, a water sample is taken from 15 m depth with a polyethylene water bottle (General Oceanics, 1.5 l). The bottle carries three digital reversing thermometers that are allowed five minutes to equilibrate before tripping. Subsamples are taken immediately for chlorophyll, macronutrients, dissolved organic carbon (DOC) and microbial community analysis, and are returned to the research station in the dark for processing. Samples generally reach the laboratory within 60 min, and in winter they are protected from freezing during transit with an insulating blanket.

2.3. Chlorophyll determination

Water samples are gently mixed by inversion and triplicate samples of 100 ml (summer) or 500 ml (winter) are then fractionated by gravity filtration through sequential 47-mm filters into the standard oceanographic size fractions, but with one extra cut to split the nanophytoplankton into larger and smaller cells:

Microphytoplankton: >20 μm (nylon mesh filter)
Large nanophytoplankton: o 20–5 μm (membrane filter)
Small nanophytoplankton: o 5–2 μm (membrane filter)
Picophytoplankton: o 2–0.2 μm (membrane filter)

Filtration and chlorophyll extraction are carried out immediately the samples are returned to the laboratory to minimise losses from chlorophyllase activity (Jeffrey and Hallegraeff, 1987), in the dark and at temperatures below 4 1C. Pigments are extracted into chloroform/methanol (Wood, 1985) and assayed by fluorometry (Turner AU-10). Fluorescence is measured, following dilution of the extract if necessary, before and after acidification with two drops of 0.1 N HCl. All fluorometry takes place in subdued light, and the fluorometer is calibrated regularly with standard chlorophyll *a* (Sigma, *Anacystis nidulans*) to establish sensitivity and the range of linear response, and the ratio of fluorescence before and after acidication is logged to monitor the reliability of the phaeopigement data. All data are reported as chlorophyll *a* (calculated as total chlorophyll—phaeopigment).

Total chlorophyll *a* (that is, chlorophyll *a* from all size fractions summed) extracted from the 15-m water samples is used to calibrate the in-line fluorometer on the CTD. The fluorometer signal is averaged over the depth range 14.5–15.5 dbar, and compared with the mean total extracted chlorophyll *a* from the water sample collected at 15 m immediately afterwards. The resultant calibration (Fig. 3) is then used to calculate the full-depth profile of chlorophyll from the CTD fluorometer data. This calibration protocol is preferred to a single-point calibration of each CTD cast because the water sample is taken immediately after the CTD cast (rather than simultaneously as typically happens from research vessels). We find that one-sample calibrations lead to unacceptable cast to cast variability in calibration, and a calibration that is strongly concentration-dependent. The use of pooled samples allows for a single calibration curve covering the entire dynamic range from very low winter (o $0.01\,mg\,m^{-3}$) to high summer concentrations ($>20\,mg\,m^{-3}$). For both fluorometers a quadratic fit explains marginally more of the variance than a linear fit, but results in a highly skewed distribution of deviations between estimated and extracted chlorophyll *a* (with the CTD underestimating high summer levels of chlorophyll *a* by as much as 50%). The linear calibration gives a better distribution of deviations, and is therefore used.

2.4. Other samples

Unfiltered samples (150 ml) are taken in glass bottles, capped with only minimal air space, and returned to UK in the dark at +4 1C. These samples, in conjunction with samples of local glacial meltwater and snowbank, are used to measure the oxygen isotope composition to determine relative contributions of sea-ice meltwater and meteoric water (glacial meltwater and precipitation) to the surface layers (Meredith et al., 2008).

A second series of samples (500 ml) are filtered (GF/C), stored in dark polyethylene bottles and returned to UK in the dark at +4 1C. These samples are analysed for macronutrients in the UK, using standard oceanographic autoanalyser protocols (Strickland and Parsons, 1968). Detection limits are 0.3 μM for nitrate, 0.1 μM for nitrite, 0.2 μM for orthophosphate, and 1.2 μM for reactive silicate (Ocean Scientific International Ltd., Petersfield, Hampshire, UK). Ammonium is measured at the research station in Antarctica, typically within 4 h of water collection. From 1997 to 2005 ammonium was assayed by the traditional indophenol technique (Solorzano, 1969) but using dichloroisocyanurate as the chlorine donor and a modified UV incubation (Catalano, 1987); calibration was by spiking of triplicate samples as described previously (Clarke and Leakey, 1996). From 2005 ammonium

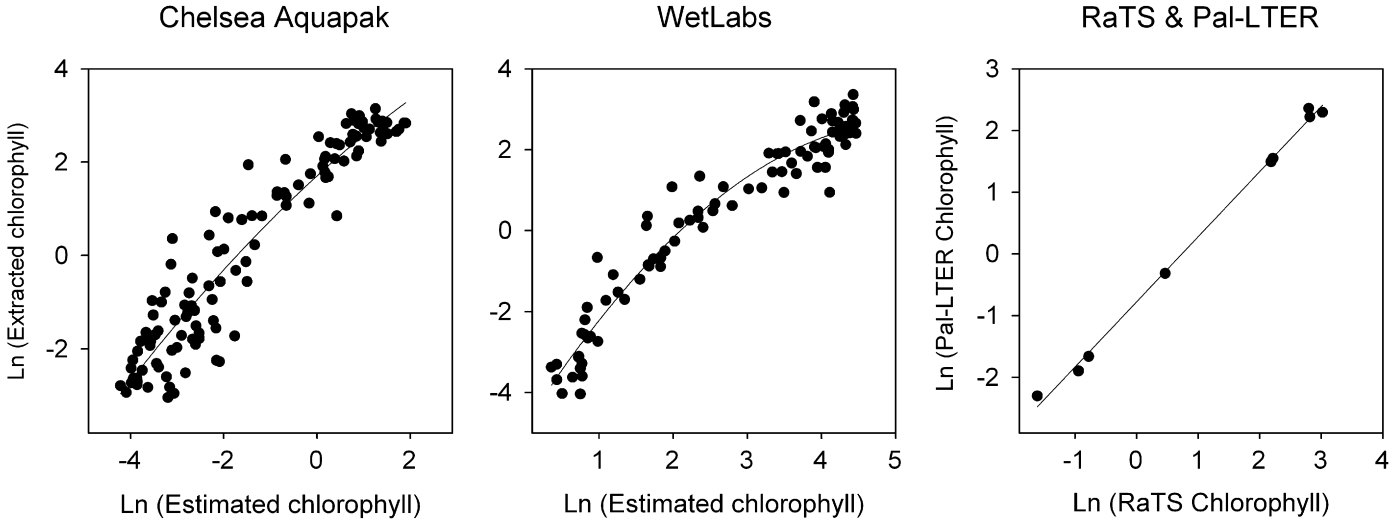

Fig. 3. Calibration of CTD fluorometers with extracted chlorophyll. Extracted chlorophyll is total chlorophyll *a* (all cells >0.2 μm) at 15 m depth; CTD chlorophyll is mean *in situ* chlorophyll *a*, averaged over depth range 14.5–15.5 dbar, as estimated from manufacturer's software and calibrations. (A) Chelsea Aquapak fluorometer. Data for events 45–277 and 341–467 ($n = 118$). (B) WetLabs fluorometer. Data for events 469–735 ($n = 95$). Note that in both instruments the very low winter fluorescence levels resulted in negative values of chlorophyll estimated using the manufacturer's calibration. These were rescaled before the calibrations were fitted to logarithmically transformed data. (C) Cross-calibration for extracted chlorophyll measured by the RaTS protocol (methanol/chloroform extraction) and the Palmer-LTER protocol (acetone extraction). Samples were taken from full-depth casts in January 2004 and 2005 to provide a wide range of values.

has been analysed with *ortho*-phthaldialdehyde (OPA) and fluorometry (Holmes et al., 1999). Samples are assayed in triplicate, and calibration is by standard addition (four concentrations, triplicate). The detection limit is 0.01 μM.

Duplicate samples for DOC are filtered through syringe filters (Whatman GD/X GMF, pore size 0.45 μM), acidified (50 μl 85% H_3PO_4 per 2.5 ml sample), and stored at −20 1C for analysis in UK. DOC concentration is measured with an MQ1001 TOC Analyser (Qian and Mopper, 1996), using in-line purging with high-purity O_2 for 2 min and high-temperature combustion. The precision and accuracy of the assay is tested daily with deep (1000 m) water from the Weddell Sea (651 37.494′S, 361 20.679′W, 607 5 μM DOC, $n = 29$, RSD 8%) and calibrated with the certified international standard deep (700 m) Sargasso Sea/Florida Straight water (467 3 μM DOC, $n = 53$, RSD 8%) from the Hansell Research Laboratory/Certified Reference Material Project (Lot 05–05, 46–47 μM). The precision (RSD) of 10 μM potassium phthalate run as sample is 13% (97 1 μM, $n = 7$) and the detection limit is 5 μM.

3. Results

3.1. Water masses in Ryder Bay

Fig. 4 shows the water mass characteristics in Ryder Bay, and illustrates their seasonal and interannual variability. UCDW is seen as the most saline water mass, with typical characteristics in the RaTS data of salinity around 34.5 and potential temperature around 1 1C. However, our sampling does not extend into the very core of UCDW, and these values are not typical of the unmodified version of this water mass.

Data from the months of the austral summer show a characteristic V-shaped inflection caused by the temperature

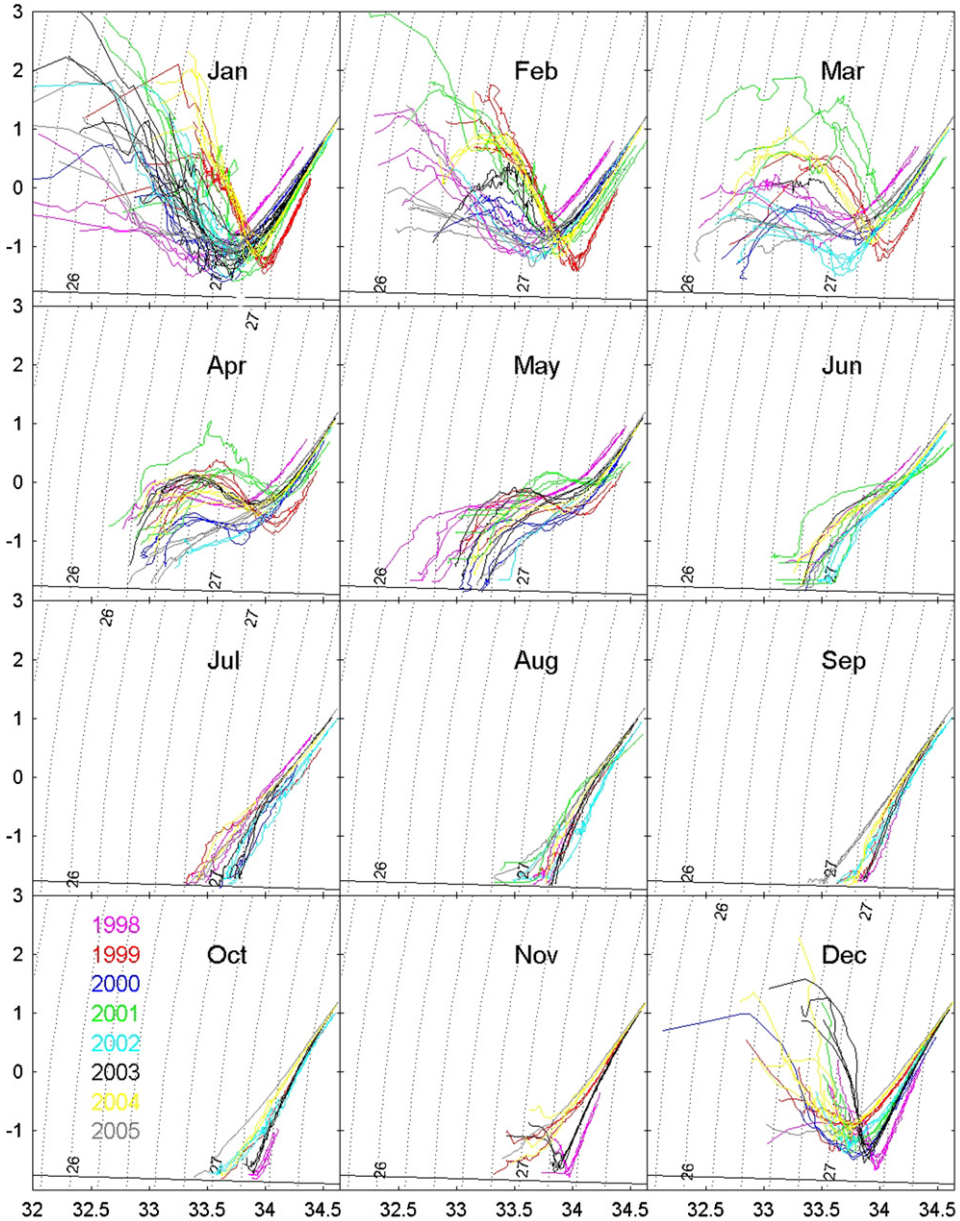

Fig. 4. Potential temperature/salinity characteristics of the waters at the RaTS station, displayed as a function of month (updated from Meredith et al., 2004). Within each month, data for each CTD cast are plotted separately.

minimum of the WW at mid-depth. Typical WW temperatures are less than −1 1C, with salinities in the range 33.4–34. The WW persists until around April or May, after which it disappears because of cooling of the surface layer. During May to June, surface temperatures reach freezing point and surface salinities increase. During July–October, the potential temperature/salinity curves are virtually straight lines between UCDW and the surface waters. This is evidence of binary mixing between mixed-layer water and the upper part of the UCDW, consistent with entrainment of UCDW into the mixed layer as this deepens. With the onset of spring, surface waters begin to warm and freshen, capping the remnant of the deep winter mixed layer, which assumes the characteristic inflection of WW.

As well as demonstrating the seasonal progression of water mass properties, the data in Fig. 4 also indicate marked interannual variability. There is considerable scatter in the temperature and salinity of the very surface layer during the summer months, reflecting significant interannual variability in heat and freshwater inputs. Although variability in WW temperatures is low, being constrained by the freezing point of seawater, the WW layer shows significant variability in its salinity, ranging from less than 33.5 in January 1998 to approximately 34.0 in January 1999.

The austral winter of 1998 is apparent as a very short line in potential temperature/salinity space; for example. This is indicative of a very deep winter mixed layer, which Meredith et al. (2004) demonstrated was the result of anomalous atmospheric and cryospheric forcing caused by the strong 1997/98 El Niño that was then decaying. The salinity of this mixed layer (and the WW it became) was anomalously high, around 34. There are indications that the 2002/2003 El Niño had a similar, but less intense impact; this is discussed elsewhere (Wallace, 2008).

A series of detailed CTD transects were undertaken in the 2004/2005 season. These transects are analysed in detail elsewhere (Wallace, 2008) and are discussed only in outline here to establish the general oceanographic context for the RaTS station. The sample design comprised major transects across the deep-water entrance to Ryder Bay, and along the longest axis of the Bay (Transects A and D in Fig. 2). The data indicate open exchange with northern Marguerite Bay, principally through the deep water opening between Rothera Point and Anchorage Island underlying Transect A. This allows modified UCDW, which originates with the ACC flooding onto the continental shelf, to bring heat and nutrients into Ryder Bay. It indicates that the data obtained from the RaTS station are likely to be representative of northern Marguerite Bay, although undoubtedly modified by local factors in some instances (for example glacial melt and local topographic control of ice and ocean dynamics).

It is possible that some water enters northern Marguerite Bay, and hence Ryder Bay, from the generally westward flowing Antarctic Coastal Current (the East Wind Drift in the older oceanographic literature), which brings water southwards along the west coast of Adelaide Island (Deacon, 1984; Longhurst, 1998; Beardsley et al., 2004; Moffat et al., 2008). The details of hydrography and water flow along the nearshore sections of the western Antarctic Peninsula continental shelf are, however, incompletely known, though it is clear that regional and small-scale oceanography is influenced strongly by gyres over the shelf (Hofmann et al., 1996).

3.2. Temperature

There is a distinct seasonal cycle in both the temperature and salinity profiles of the surface mixed layer in Ryder Bay (Fig. 5). Surface waters are warmed by absorption of solar radiation from November to January, although the timing can vary from year to year depending on the presence of ice. Peak temperature is typically in late January, though there can be smaller peaks later in the season. Isotherms deepen as heat is lost to the atmosphere and brine is rejected into the upper ocean as ice is formed in early winter (April–July). From July to October surface temperatures are typically close to, and often at, the freezing point of seawater.

At the 15 m reference depth, the seasonal cycle is very clear (Fig. 6A), with winter minima close to the freezing point and summer peak values typically in the range 0.3–1.7 1C. For an organism living within the surface waters the seasonal variation in temperature, although small in comparison with temperate latitudes, is important. The range of this seasonal variation is strongly depth-dependent with the annual range being greater closer to the surface (Fig. 6B). This variation means that the rate of any physiological process, such as growth or the development of reproductive tissue, will differ with depth. The variability in temperature reaches a minimum value at ~100 m. At this depth the overall range of temperatures in the data set is −1.81 to +0.46 1C, but there is no correlation with temperatures higher in the water column (15 versus 100 m, Pearson $r = 0.041$, $P = 0.477$), indicating different sensitivities at these depths to the range of processes that control oceanic temperature. Below ~100 m variability in temperature increases, caused by intermittent flushing and vertical mixing of UCDW below the thermally more stable WW layer. These processes lead to an increase in temperature variability over the depth range 100–160 m; below this depth temperature variability is once again greatly reduced in the fairly stable modified UCDW.

In addition to the marked seasonality, the temperature of the AASW also varies between years (Figs. 5A and 6A). At the 15 m reference depth at the RaTS station in Ryder Bay summer peak temperatures exceeded +1.5 1C in three seasons (January 1999, 2001 and 2004) but in others never exceeded +0.5 1C (austral summers 1999/2000, 2001/2002 and 2004/2005) (Fig. 6A). In the very topmost waters solar heating on calm sunny days can raise the temperature above 5 1C in northern Marguerite Bay (for example in January 2001: unpublished BAS observations).

There are also clear seasonal signals in the salinity data (Fig. 5B). The surface layers are typically freshest from January to April, as a result of the melt of sea-ice cover from the previous winter coupled with input from glacial meltwater. The onset of winter ice formation raises surface salinity as a result of brine rejection, and this typically starts in May or June.

3.3. Mixed-layer depth

The density structure of the water column (controlled by salinity and, to a much smaller extent, temperature) determines the mixed-layer depth (MLD), which is of profound significance to primary production (Sverdrup, 1953). MLD is calculated using the potential density anomaly, σ_0, where $\sigma_0 = \rho - 1000$ and ρ is the density in kg m^{-3}. Following Barth et al. (2001) we estimate MLD as the depth at which $\sigma_0 = \sigma_0(\text{surface}) + 0.05$. When averaged over the entire data series, MLD shows a strong seasonal signal (Fig. 7A). MLD is shallow in summer, and then deepens as a result of the increase in surface density associated with brine rejection from winter sea-ice, coupled with an increased mean wind speed in winter. MLD typically reaches its maximum in August, and thereafter shallows towards spring.

Although the long-term (climatological) mean winter maximum MLD is ~60 m, this figure masks considerable interannual variability (Fig. 7B). Winter mixing was particularly deep

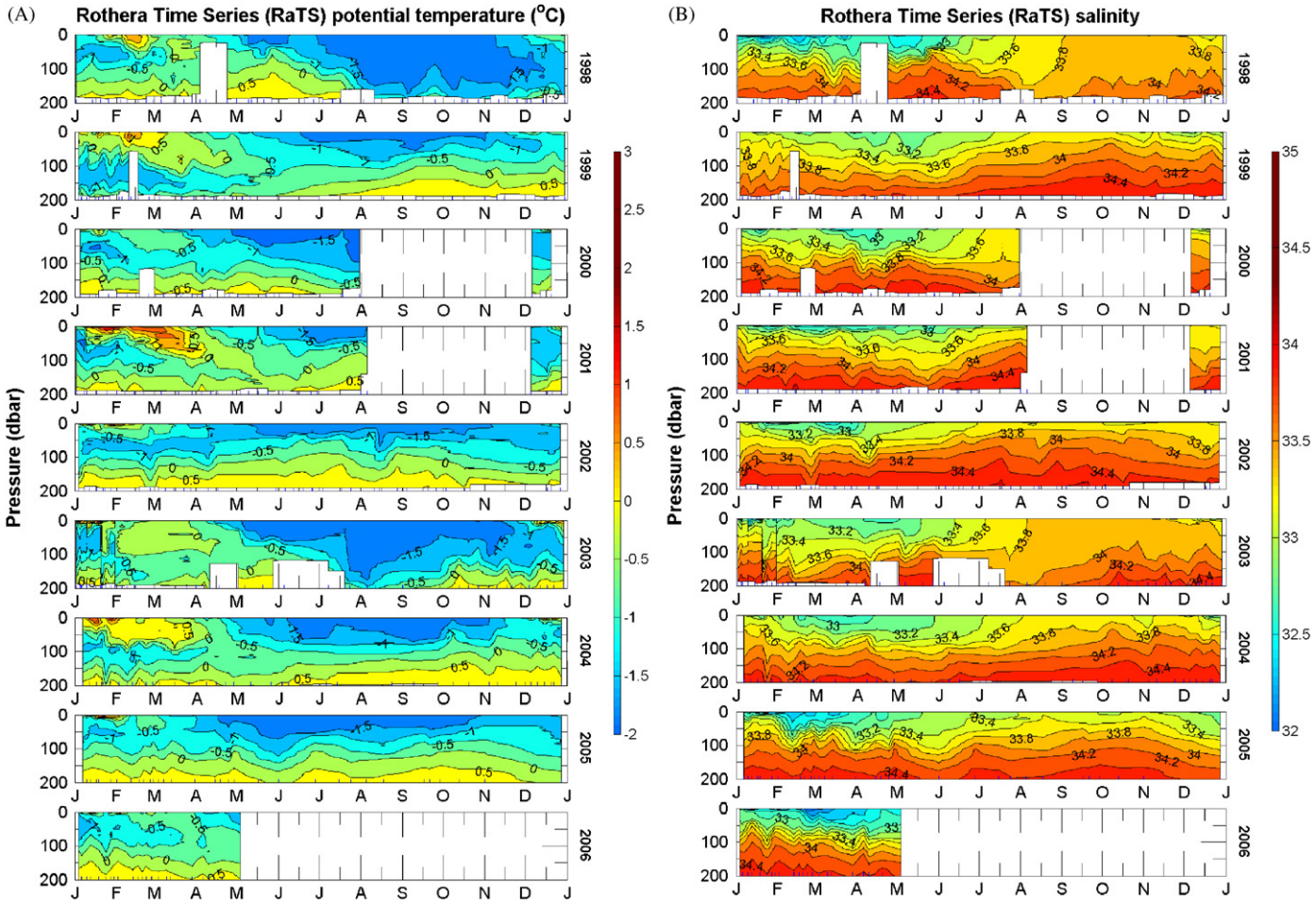

Fig. 5. Time series of temperature and salinity for the uppermost 200 m at the RaTS station. (A) Potential temperature. (B) Salinity. Data are plotted by calendar year so that the important winter period falls in the centre of the plot.

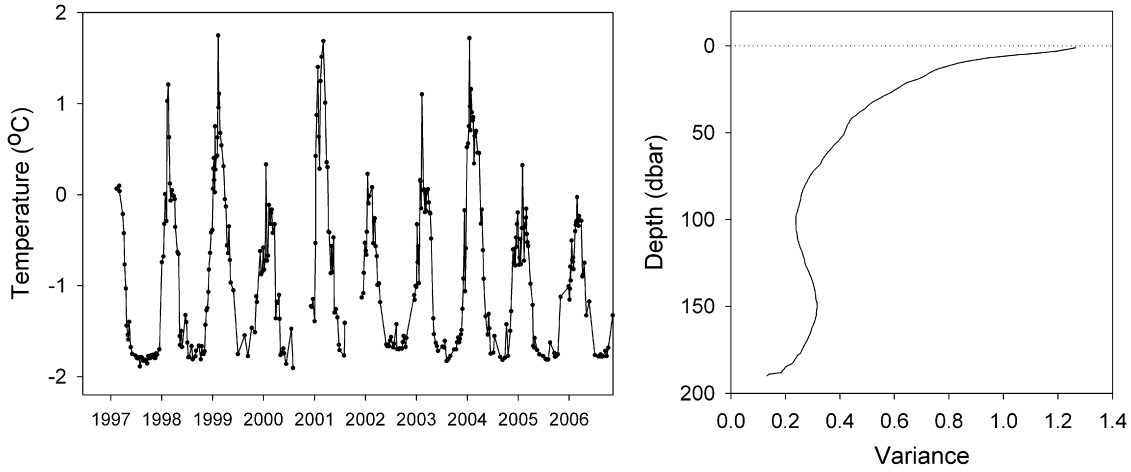

Fig. 6. Seasonal and inter annual variation in temperature within the mixed layer, Ryder Bay, 1997–2006. (A) *In situ* temperature at 15 m depth. (B) Variance in temperature with depth at RaTS station in Ryder Bay. Variance calculated for complete data series, averaged over bins of 1 dbar.

in 1998 and 2003. The 1998 event was associated with the very strong 1997/98 El Niño, and was driven by intense regional sea-ice formation (Meredith et al., 2004), while the deep mixed layer in 2003 was associated with the moderate 2002/2003 El Niño (Wallace, 2008). In other years winter mixing typically extends only to 40–60 m, and in 1999 the winter MLD reached only ~30 m.

3.4. Ice

Winter fast-ice in Ryder Bay has been extremely variable in both timing and duration since the start of the RaTS programme in 1997. In some winters (1997, 2002, 2005) fast-ice was present continuously for >200 days; in others it was highly intermittent. In 2001 ice was rarely present for more than a few weeks, and this

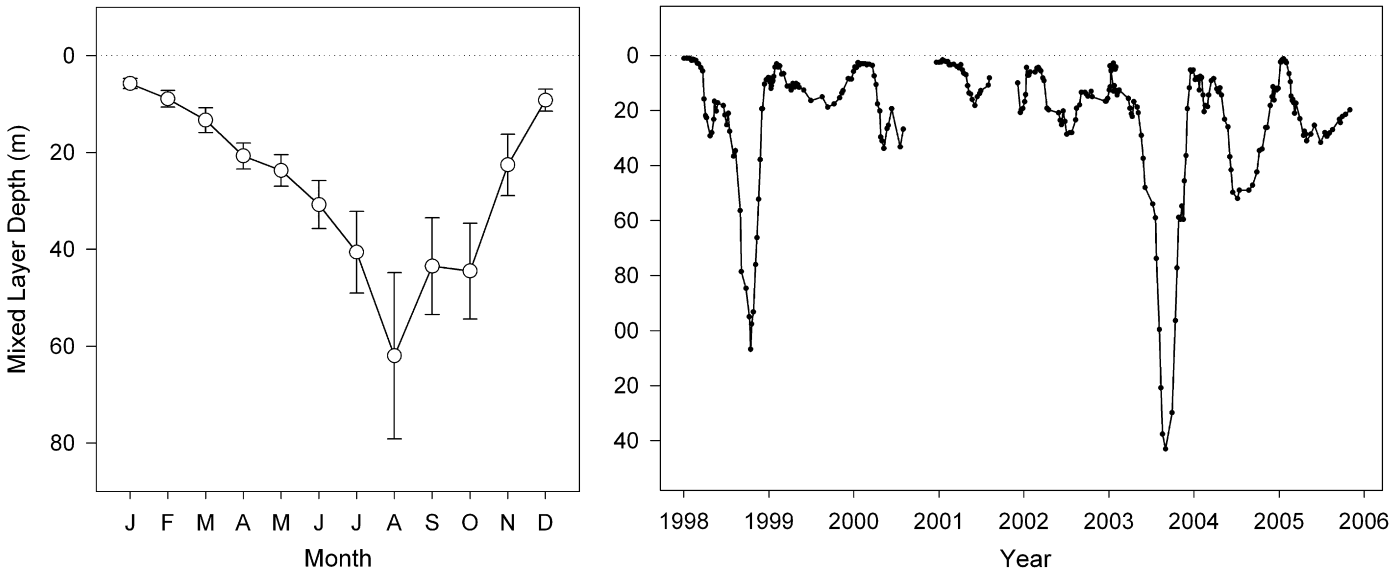

Fig. 7. Mixed-layer depth at RaTS station, Ryder Bay, northern Marguerite Bay. (A) Annual climatology: all data for period 1997–2006 pooled by month. Note that data are plotted as calendar year (January–December) so that the important austral winter period lies in the centre of the plot. (B) Interannual variability for 1997–2006. Data plotted as five-point running mean to eliminate short-term noise. Note the particularly deep winter mixing in 1998 and 2003, associated in both cases with the decay of an El Niño event.

was followed by an anomalous summer season (Massom et al., 2006). Ice typically blows out in a northerly storm following a period of warm weather, and this may not take place until well into December after a period of extended winter fast-ice.

3.5. Light and compensation depth

The traditional definition of the base of the surface euphotic zone is the depth where photosynthetically active radiation (PAR) falls to 1% of the value immediately below the ocean surface. Because of the extreme seasonality of photoperiod and irradiance flux at high latitudes, together with the confounding effect of surface ice and surficial snow, we have instead estimated the depth of net photocompensation irradiance (NPI), the value of PAR which results in a net phytoplankton growth rate of zero, in the presence of most naturally occurring losses. We have taken NPI to be 15 $\mu E\,m^{-2}\,s^{-1}$, based on measurements made in the Bellingshausen Sea (Boyd et al., 1995).

As would be expected, NPI depth varies seasonally, and the long-term average maximum for Ryder Bay is ~30 m in October (Fig. 8A). This corresponds to the time of year when winter fast-ice has often departed, and the water-column bloom has yet to develop. As the spring bloom develops, NPI depth shallows to about 10–12 m where it lies for most of the summer. In the depths of winter, when incident radiation is almost non-existent and what light does exist is often reduced by fast-ice, NPI depth reaches the surface. There is also marked interannual variability in NPI depth (Fig. 8B). Maximum values range from o 20 m to >40 m, though values during the summer phytoplankton bloom are typically ~10 m.

3.6. Total chlorophyll a

The annual cycle of algal chlorophyll *a* at the RaTS station in Ryder Bay shows the typical high-latitude pattern of a well-defined summer phytoplankton bloom combined with a long winter period of very low chlorophyll levels (Fig. 9). The bloom typically reaches peak values in December and January, and the climatology suggests a secondary late summer bloom in March. The bloom is shallow, with peak chlorophyll *a* levels above 20 m, though the bloom does extend to ~60 m.

The climatology exhibits a relatively simple structure which masks considerable interannual variability in the timing, intensity and depth of the bloom (Fig. 10). In 1997/98 there was a single bloom with a well-defined January peak, whereas in the 2000/2001 season the bloom was extended in time over the entire summer from late November to late March with at least three separate peaks in total chlorophyll. The 1998/99 season had a relatively shallow bloom, rarely extending deeper than 40 m, whereas the 2001/2002 season bloom extended to 60 m and late in the 2003/2004 season the bloom showed a steady deepening from late January to late March.

This strong interannual variability is evident in the data for total extracted chlorophyll at the 15 m reference depth at the RaTS station (Fig. 11A). These samples come from a depth representing the long-term (climatological) peak of the bloom and typically reach maximum levels of 20–25 $mg\,m^{-3}$, although individual years can be lower (2001) or higher (2003). These are intense blooms, and the peak values are typical of those reported for nearshore waters elsewhere in Antarctica (Hart, 1934; Bunt, 1960; Mitchell and Holm-Hansen, 1991; Clarke and Leakey, 1996). Because the 15-m reference depth typically lies within the most intense bloom, chlorophyll *a* levels here are strongly correlated with total water-column chlorophyll *a* integrated to 50 m (Fig. 11B) and 100 m (data not shown). Mean total water-column chlorophyll *a* (integrated to 100 m, pooled by week for all data 1998–2006) typically exceeded 0.2 $g\,m^{-2}$ for the period from mid-November to late March. Seasonal peak values varied from 0.57 $g\,m^{-2}$ in 1997/98 to 1.34 $g\,m^{-2}$ in the 2001/2002 season.

A chlorophyll *a* time-series can also be constructed from CTD fluorometer data by averaging *in situ* fluorescence between 14.5 and 15.5 dbar, and applying the calibration curve erected

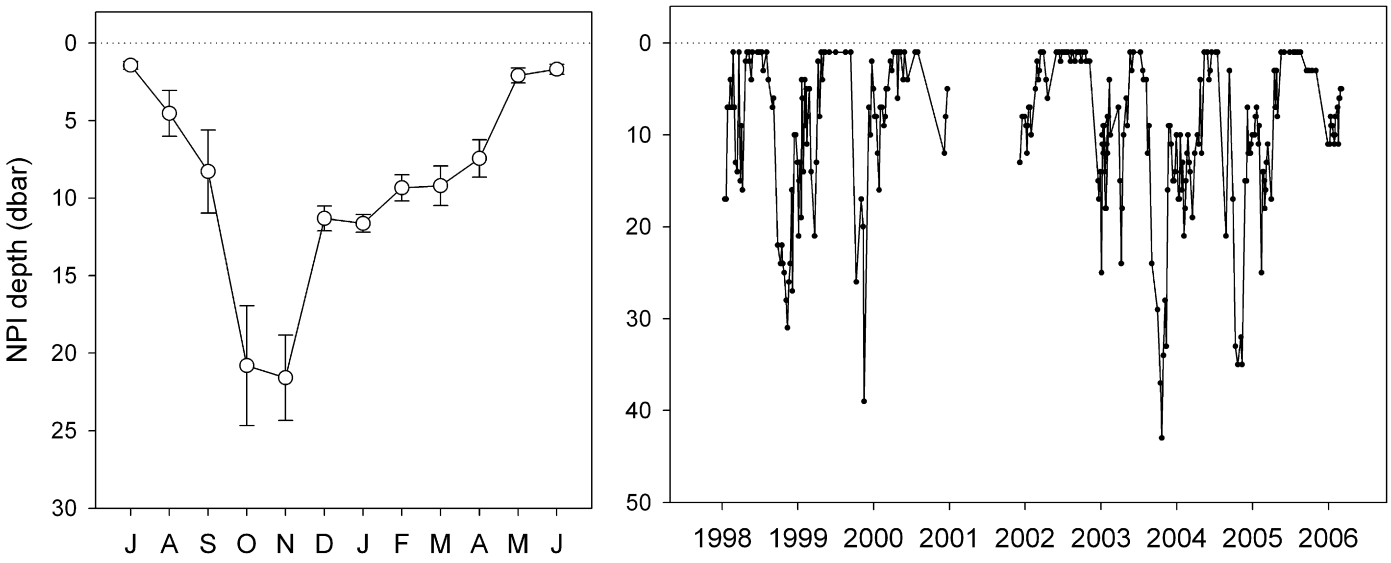

Fig. 8. Seasonal and interannual variation in the depth of net photocompensation irradiance (15 μE m^{-2} s^{-1}). (A) Annual climatology: all data for 1997–2006 pooled by month. Note that data are plotted from midwinter (July) to midwinter (June) so that the austral summer season lies in the centre of the plot. (B) Interannual variability for 1997–2006.

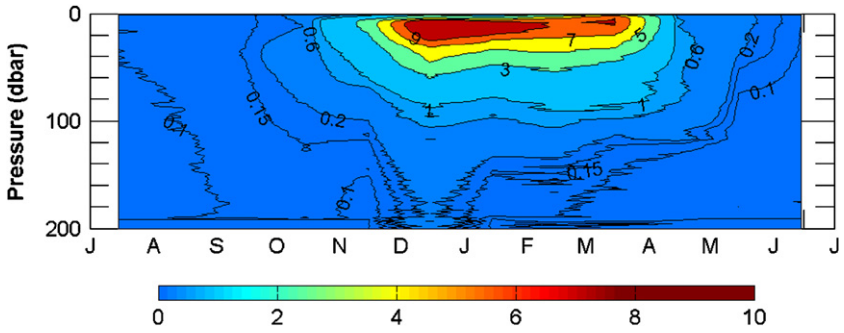

Fig. 9. Seasonal progression of the phytoplankton bloom in surface waters at the RaTS station, Ryder Bay. Data are from CTD fluorometer, calibrated with extracted chlorophyll *a*; contours are scaled to emphasise detail at low chlorophyll levels. Annual climatology: all data for 1997–2006. Note that data are plotted from midwinter (July) to midwinter (June) so that the austral summer season lies in the centre of the plot. The bulk of the bloom is confined to depths shallower than ~50 m. Note the indication of vertical flux shown by the deepening of the concentration contours from late November to late January, and the indication of a late summer bloom in March.

from extracted chlorophylls taken at the same time (shown in Fig. 3 for both the Chelsea and WetLabs fluorometers). Comparison of the two time-series showed that differences were small and showed no systematic trend, apart from a tendency for *in situ* fluorescence to overestimate chlorophyll *a* compared with extracted chlorophyll in spring when the bloom is growing rapidly.

3.7. Size-fractionation

Weekly samples taken from the 15 m reference depth at the RaTS station are fractionated at 20, 5, 2 and 0.2 μm. As expected, the microplankton fraction (>20 μm), comprising large solitary or chain-forming diatoms together with a range of unidentified colonial forms, dominates the summer bloom (Fig. 12A). The microplankton bloom typically starts in early November, reaching peak concentrations through December to January, declining to reach winter levels again in April. Although when averaged over the entire data series (1997–2006), summer microplankton chlorophyll *a* levels fall in the range 8–13 mg m^{-3}, peak levels in individual years typically exceed 20 mg m^{-3} for short periods.

3.8. Nanoplankton chlorophyll

Both nanophytoplankton fractions show a strong seasonality but this is most marked in the larger fraction (o 20–5 μm). These cells show a similar seasonality to the microplankton, though typically peak levels are an order of magnitude lower and are reached later in the season (Fig. 12B). The smaller nanoplankton fraction (o 5–2 μm) exhibits a far less marked seasonality, increasing slowly above winter levels from September and reaching peak levels in late summer that are roughly an order of magnitude lower than the larger fraction. Both blooms drop away sharply in early March, and then decline more slowly to a midwinter minimum in July/August.

3.9. Picoplankton chlorophyll

Chlorophyll *a* in the picoplankton fraction (o 2–0.2 μm) is only moderately variable, occasionally below detection, and typically an order of magnitude less than nanoplankton in concentration (Fig. 12A). The picoplankton fraction shows a small degree of seasonality: when pooled by week chlorophyll peaks at 0.07 mg m^{-3} in spring (early November) and 0.06 mg m^{-3}

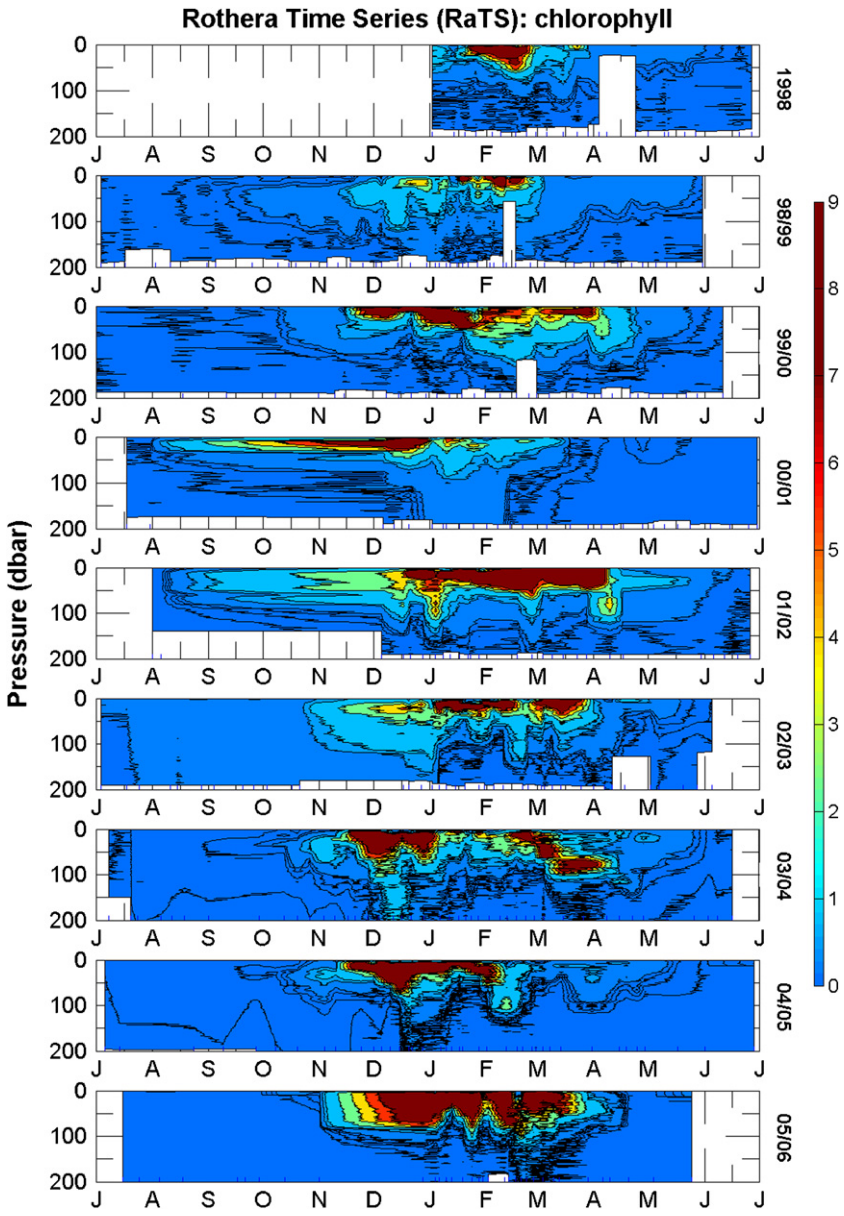

Fig. 10. Interannual variability in total chlorophyll *a* in surface waters at the RaTS station, Ryder Bay. Data from CTD fluorometer, calibrated with extracted chlorophyll. Note that data are plotted from midwinter (July) to midwinter (June) so that the austral summer season lies in the centre of the plot.

in high summer (mid-January). Picoplankton chlorophyll is at winter levels (o $0.01\,mg\,m^{-3}$) through June to August, but starts to increase in September, before any of the larger size fractions.

3.10. Seasonal changes in phytoplankton size fractions

Winter chlorophyll *a* levels in Ryder Bay are typically very low, with an average concentration o $0.01\,mg\,m^{-3}$ for both the microplankton (>20 μm) and picoplankton (o 2–0.2 μm) fractions (Fig. 13A). For the two nanoplankton fractions winter chlorophyll levels are markedly higher, exceeding $0.02\,mg\,m^{-3}$ for the larger (o 20–5 μm) fraction (Fig. 13A). In summer and autumn the total chlorophyll is dominated by the microplankton (>20 μm) fraction (Fig. 13B).

In Ryder Bay the annual mean values for percentage microplankton (>20 μm) and nanoplankton (o 20–2 μm) are 50% and 43%, respectively, whereas during the summer bloom period microplankton increases to 90% of total chlorophyll *a*. As would be expected, the relative proportions of the main size fractions in spring and autumn are intermediate between winter and summer. These figures are not straightforward to interpret, neither are they easy to compare with other data. This is because the values represent the relative balance of an intense bloom of large cells and colonial forms in summer superimposed on a longer but less intense bloom of flagellate cells and smaller diatoms. These different seasonal dynamics mean that calculations of percentage contribution from different size fractions will be highly dependent on the time of year, the period over which data are averaged, and the intensity of the microplankton bloom. Comparisons between different seasons or locations are therefore better undertaken using absolute concentration data (Fig. 13A and B).

3.11. Coupling primary production to the rest of the food web: flux and DOC

Carbon fixed by primary producers in the ocean passes to the rest of the food-web through three primary routes: by grazing

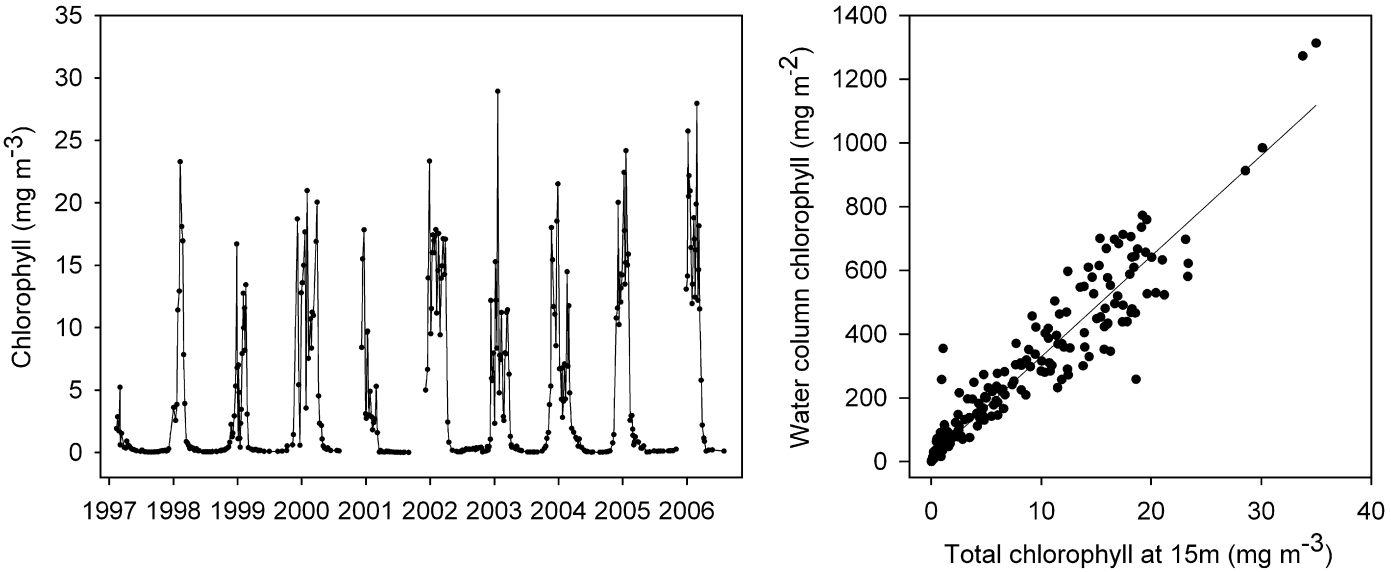

Fig. 11. Total chlorophyll *a* at the RaTS station, Ryder Bay. (A) Extracted chlorophyll *a* (total: all size fractions combined) at 15 m depth. (B) Relationship between chlorophyll concentration at 15 m and total water-column chlorophyll *a* integrated to 50 m. Data for January 1998 to February 2006 ($n = 311$, Po 0.001).

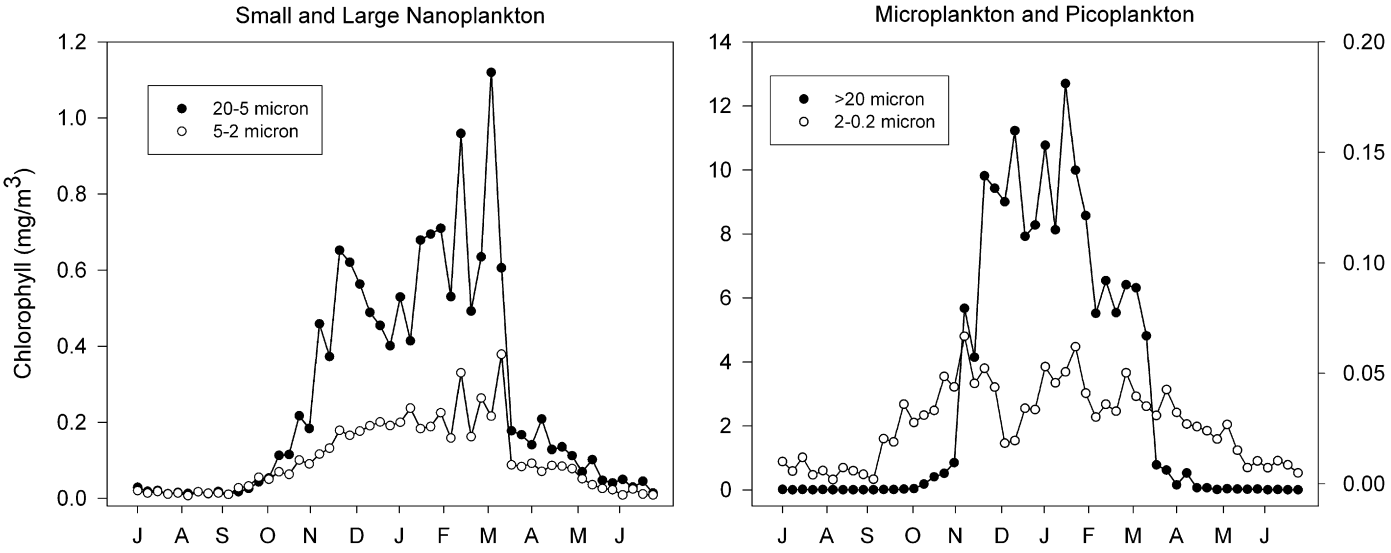

Fig. 12. Size-fractionated chlorophyll *a* at the RaTS station, Ryder Bay. Data are for 15 m, and are pooled by week and averaged over 1997–2006. Note that data are plotted from midwinter (July) to midwinter (June) so that the austral summer season lies in the centre of the plot. (A) Nanoplankton, with larger (o 20–5 μm) and smaller (o 5–2 μm) fractions plotted separately but to the same scale. (B) Microplankton (>20 μm, left-hand scale) and picoplankton (o 2–0.2 μm, right-hand scale). Note the very different scales for these two plots.

to suspension feeders within the mixed layer (and thereby to carnivores and their predators), by flux to the benthos, and to the microbial network (Ducklow et al., 2006; Clarke et al., 2007).

Flux was not measured in this study but the timing of the main period of phytodetrital sedimentation can be estimated from the presence of marked spikes in the fluorescence profile below the mixed layer. Data are available for three austral summer seasons when CTD casts were sufficiently deep. The period of flux was 18 days in 2003/2004 (4–22 December) and 23 days in 2004/2005 (21 December–13 January). The later flux in 2004/2005 compared with 2003/2004 matches a later microplankton bloom in that year. In 2005/2006 there were two periods of flux, 4–13 January and 17 February–13 March, the main period being much later than in the previous 2 years. This matches closely the pattern established for the WAP continental shelf, where over the period 1993–2005 show a sharp annual pattern, with flux lasting 50–100 days and a peak typically in January (Ducklow et al., 2006).

In some polar areas, melting of winter fast-ice releases large quantities of ice algae and associated microbial biota that can sediment rapidly to the seafloor (Thomas and Dieckmann, 2003). In Ryder Bay the winter ice typically blows out rather than melts *in situ*. In consequence the late winter–early spring ice-associated community is taken out into northern Marguerite Bay, rather than sedimenting to the seabed within Ryder Bay. Exceptions to this were the winters of 2000 and 2006, when the ice remained in Ryder Bay well into spring. Significant melting of this ice resulted in a large dump of phytodetritus, which carpeted the seabed in shallow waters for some weeks.

Whereas carbon is transferred to water-column grazers or benthos in particulate form as intact cells, aggregates or faecal pellets, transfer to the microbial network is in the form of

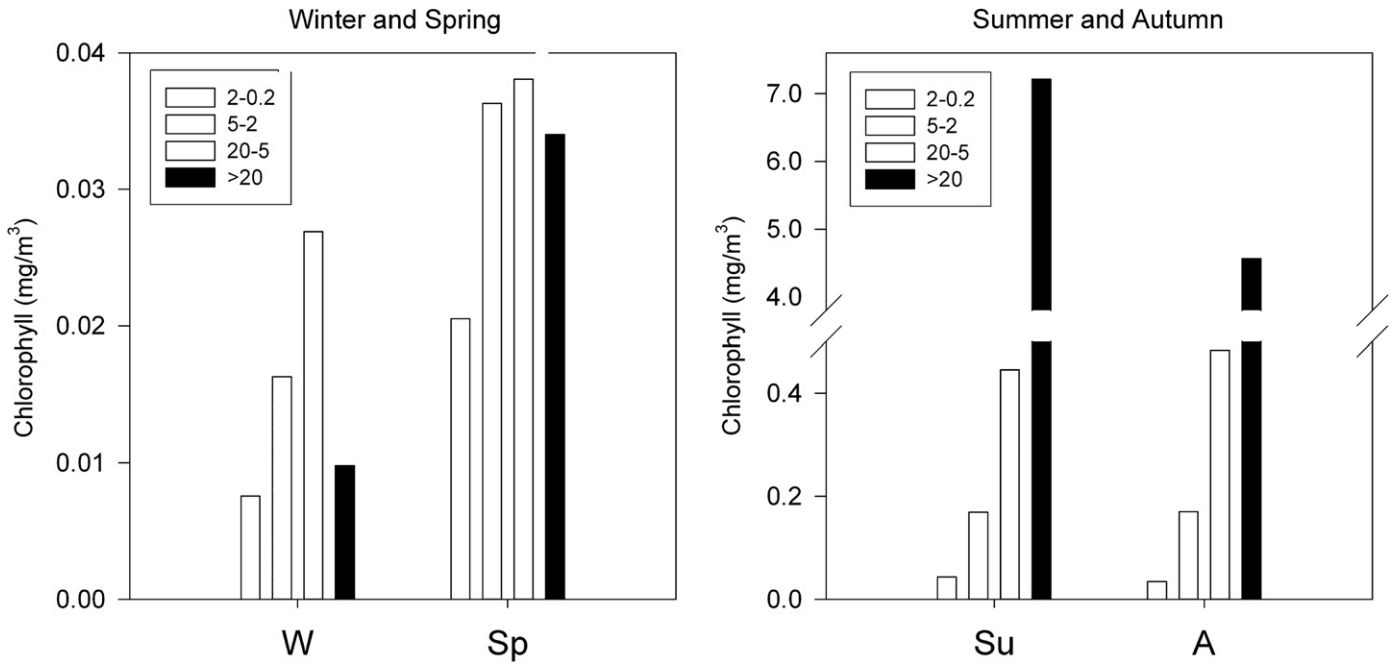

Fig. 13. Seasonal variation size-fractionated chlorophyll *a* from 15 m depth at the RaTS station, Ryder Bay. (A) Data for winter (June–August) and spring (September and October). Note that in these seasons the concentration of chlorophyll *a* both the large (o 20–5 μm) and small (o 5–2 μm) nanoplankton fractions exceed that of the microplankton (>20 μm). (B) Data for summer (November–January) and autumn (February–May). Note the different scale for microplankton.

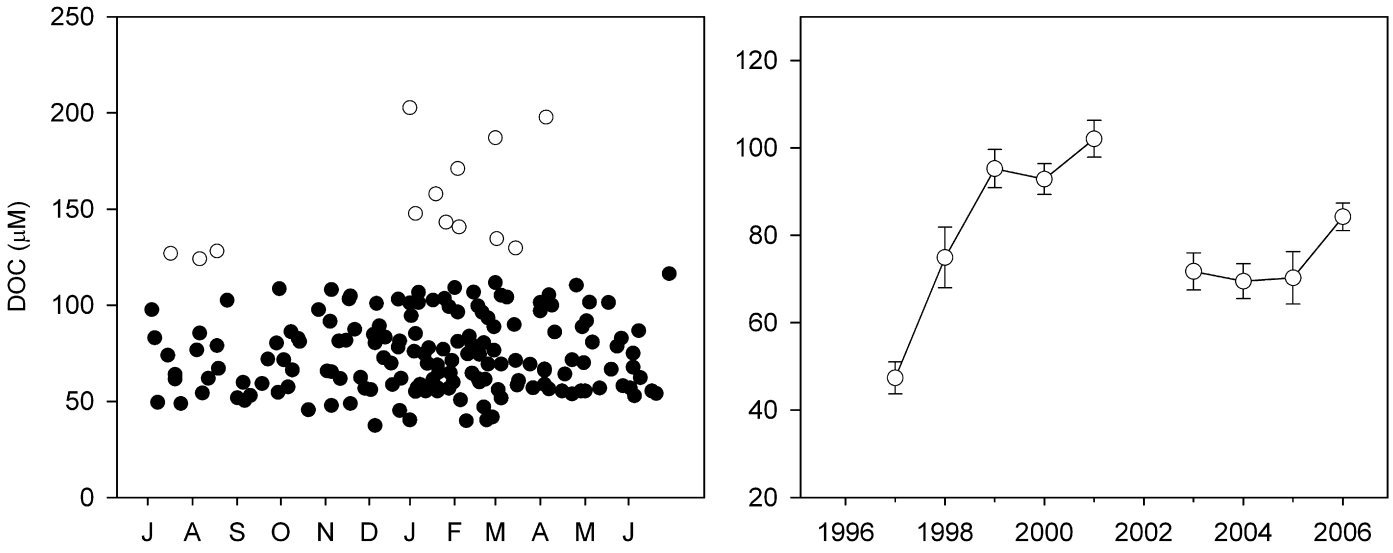

Fig. 14. Dissolved organic carbon (DOC) at the RaTS station, 1997–2006. (A) All data (black symbols), with a small number of suspect high data shown as open symbols. Note that data are plotted from midwinter (July) to midwinter (June) so that the austral summer season lies in the centre of the plot. (B) Mean data for the summer period (November–March) plotted as a function of year. Number of data points range from 2 (2000) to 17 (2006). Missing data were caused by the loss of samples in a laboratory fire in 2001, and inability to sample in periods of bad weather or ice.

dissolved organic matter. DOC is highly variable at the RaTS station (Fig. 14A). Minimal levels are in the range 40–50 μm, which are typical values for the refractory component of organic carbon in the global ocean (Wedborg et al., 1998; Carlson and Hansell, 2003). Although summer values tend to be higher, there is no significant seasonal signal (one-way ANOVA, data pooled by month, $F = 0.69$, $P > 0.05$). Neither is a broad winter/summer comparison significant ($F = 0.72$, $P > 0.05$). Comparison of summer (November–March) data alone, however, reveals a highly significant interannual variability ($F = 7.49$, Po 0.001) (Fig. 14B). These data suggest the existence of a labile and dynamic pool of DOC superimposed upon a more refractory background. At least some of this variability may be related to release of DOC-rich brines from overlying sea ice when this is present (Thomas et al., 2001; Carlson and Hansell, 2003).

3.12. Macronutrients

The concentration of ammonium, nitrate, nitrite and orthophosphate at 15 m at the RaTS station all exhibit a clear seasonal cycle (Fig. 15).

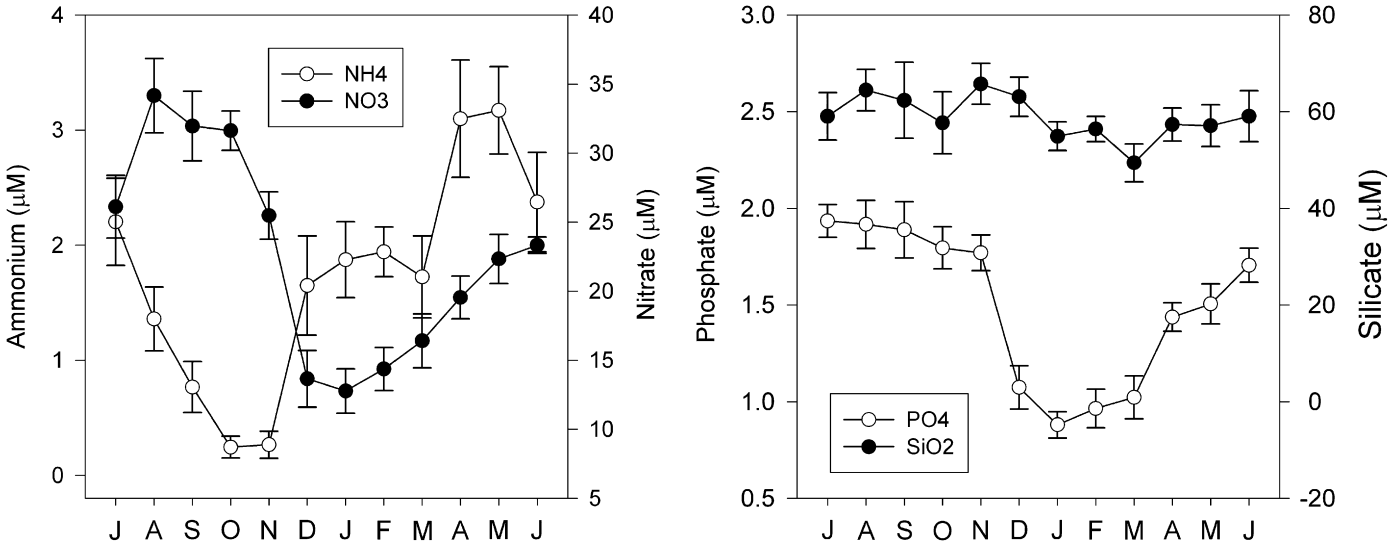

Fig. 15. Seasonal variation in macronutrients at the RaTS station, 1997–2005. All data pooled by month. Note that data are plotted from midwinter (July) to midwinter (June) so that the austral summer season lies in the centre of the plot. Note also the different scales for each nutrient. Data plotted as mean7 SE. (A) Ammonium and nitrate and (B) orthophosphate and reactive silicate.

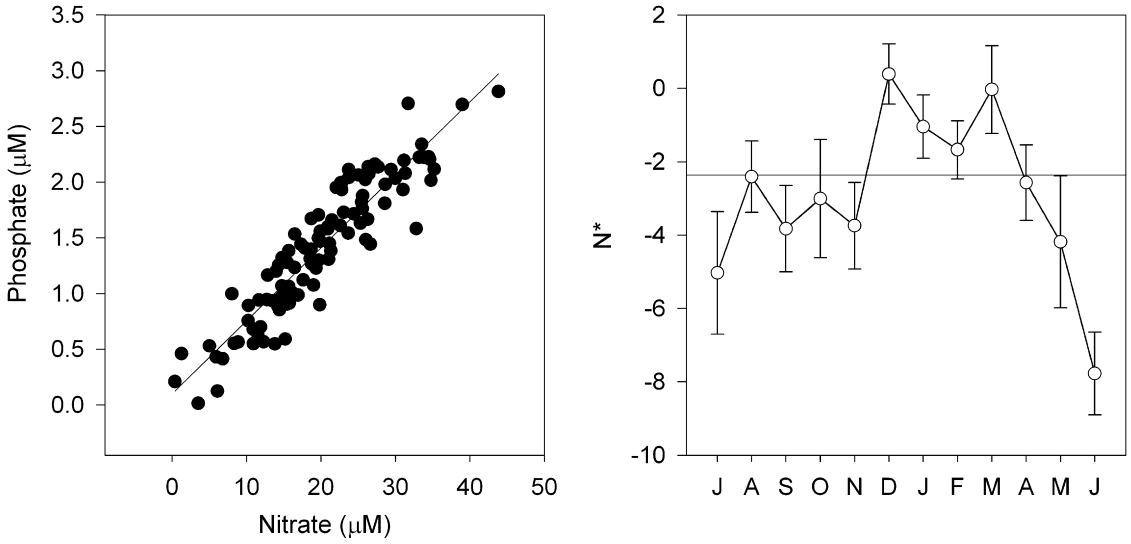

Fig. 16. Stoichiometry of N and P utilisation at the RaTS station. (A) Covariation plot for phosphate and nitrate showing tight correlation ($n = 103$; Po 0.001) between the concentration of these two macronutrients at 15 m. Data are for all seasons over the entire RaTS period (January 1997–February 2005). (B) Seasonal variation in the quasi-conservative tracer N^*, calculated as $N^* = [NO_3{+}NO_2]-16[PO_4]$, where all concentrations are μM. Data are for all RaTS events where all three macronutrients were measured on the same water sample; data are plotted as mean7 SE, pooled by month. Note that the data are plotted from midwinter (July) to midwinter (June) so that the austral summer lies in the centre of the plot. The horizontal line shows the overall mean value of N^* for the complete data set (−2.37).

Nitrate reaches a peak value of ~35 μM in midwinter (August). Utilisation of nitrate begins in early spring and concentrations decline rapidly from October to December (Fig. 15A). Minimal levels, typically o 15 μM, are observed throughout the rest of the summer, and thereafter nitrate concentrations climb steadily back to the winter peak value. A clear seasonal pattern related to utilisation by the spring and summer phytoplankton bloom is also shown by phosphate (Fig. 15B). Phosphate levels are highest in the middle of winter, typically approaching a maximum of ~2 μM in July. There is some indication of slow utilisation of phosphate in winter but concentrations decline rapidly from November to January, with the seasonal minimum typically o 1 μM; phosphate concentrations then rise steadily from January to July.

Concentrations of nitrate and phosphate are tightly coupled (Fig. 16A; $F = 587$, Po 0.001), with the slope (15.3), indicating stoichiometry close to Redfield. The 95% confidence intervals (14.1–16.6) encompass the mean global value of 167 1 established by Anderson and Sarmiento (1994). The quasi-conservative tracer N^* (Gruber and Sarmiento, 1997), calculated here in its simplified form where $N^* = (NO_3{+}NO_2)-16(PO_4)$, has an overall mean value of −2.37. It does, however, exhibit a strong seasonal signal at the RaTS station, with values greater than the mean in summer (December–March) and a strong decline from March to June (Fig. 16B). Variability in N^* at the RaTS station is driven principally by phosphate, and the sharp decline in autumn and winter marks the period when phosphate concentrations are climbing relatively faster than nitrate.

A very different seasonal pattern is exhibited by ammonium (Fig. 15A). Here concentrations peak in autumn/early winter (April–May) with average concentrations >3 μM, and individual

values exceeding 5 μM. Ammonium concentrations then decline steadily through winter, reaching minimum values in spring (October–November). Mean values at this time are o 0.3 μM, and ammonium is frequently undetectable. Concentrations then rise throughout the summer, and again in autumn.

Concentrations of reactive silicate are somewhat variable, but they do exhibit a marked decline from a maximum value >65 μM in November to a seasonal minimum o 50 μM in March (Fig. 15B). Thereafter concentrations increase to midwinter (July), though there are indications of a late winter/early spring decline from August to October. The main period of silicate utilisation corresponds with the development of the summer phytoplankton bloom, though, interestingly, it is later than the nitrate decline by 1–2 months. Silicate and nitrate covary in the RaTS data set ($F = 17.85$, Po 0.001) with the slope of the covariation plot indicating a stoichiometric utilisation ratio of 1.67 (95% CL 1.12–3.23).

4. Discussion

The potential temperature and salinity data indicate that the water masses observed in Ryder Bay are the same as those that characterise the continental shelf of the western Antarctic Peninsula (WAP) and Marguerite Bay. The major differences from the more open continental shelf are the greater influence of surface glacial meltwater and the different regional dynamics of ice production in winter because of the combined influence of local topography and meteorology (Meredith et al., 2004). There is also the likelihood of a greater modification of UCDW because of the larger distance over which this water travels to reach Ryder Bay from the ACC at the edge of the continental shelf, and hence the longer time for interaction with the overlying AASW. The data, however, do indicate that the dominant processes determining the dynamics of the water column in Ryder Bay are similar to those operating on the WAP continental shelf. Year-round data collected at the RaTS station thus have much to contribute to our understanding of the oceanography of the WAP continental shelf in general.

4.1. The seasonal cycle in Ryder Bay

All features of the physical, chemical and biological oceanography in the surface waters of northern Marguerite Bay exhibit the expected strong seasonality. Of particular ecological relevance are the seasonal variation in temperature and chlorophyll.

At the RaTS station temperature varies from a winter minimum close to the freezing point to a summer maximum, which can be o 0.5 1C or >1.5 1C (Fig. 6A). The extent of this variability is strongly depth-dependent (Fig. 6B), and the thermal environment experienced by an organism will therefore depend on its position in the water column. This applies both to sessile benthic organisms and to actively migrating zooplankton or fish. A benthic organism living at 20 or 50 m will experience a strong and predictable seasonality in temperature, whereas one living at 100 m would be subject to a far less predictable and less extensive variation; at depths below 200 m temperatures are seasonally stable, with thermal variability driven principally by episodic flooding of UCDW into the continental shelf. Many features of the ecology of benthic organisms, such as their growth or reproductive biology, will thus be strongly depth-dependent, and autoecological studies undertaken at the shallow depths available to SCUBA sampling will not necessarily reflect the ecology of even the same species living on the deep continental shelf.

At the RaTS site the phytoplankton bloom usually starts in November (Fig. 9), which is typically when the mean depth of net photocompensation irradiance (NPI) crosses the rapidly shallowing base of the mixed-layer. This is usually when chlorophyll a concentrations first exceed 1 mg m^{-3}, and hence the long-term mean picture matches the classical model of the initiation of the vernal phytoplankton bloom (Sverdrup, 1953). The bulk of the chlorophyll is, however, at or below 15 m for most of the summer, which is below both NPI depth and the MLD for this time. Furthermore the bloom stays at concentrations well above 1 mg m^{-3} for almost a month after the MLD drops below NPI depth, which typically is in February. Neither is there any relationship between the duration, timing or depth of the bloom with either MLD or NPI depth when examined on a year-by-year basis (all $p > 0.05$). The annual cycle of the phytoplankton bloom in northern Marguerite Bay thus indicates that, as others have concluded (Mitchell and Holm-Hansen, 1991; Obata et al., 1996), the classical critical depth theory for the development of the summer bloom is incomplete for high southern latitudes. Using data from the RACER (Research on Antarctic Coastal Ecosystem Rates) study on the northern WAP shelf, Mitchell and Holm-Hansen (1991) concluded that intense phytoplankton blooms could only develop when the MLD was o 25 m. This modelling study assumed no limitation by nutrients, and also that loss rates from grazing or flux were large (of the order 0.3–0.35 day^{-1}). An extended year-round data set of water-column physics and phytoplankton bloom dynamics, such as that provided by the RaTS project, will allow future critical tests of models of primary production in high-latitude waters.

The summer phytoplankton bloom in Ryder Bay is dominated in biomass by large diatoms and a variety of colonial cells including haptophytes and chain-forming diatoms. For the RaTS data series overall there is a very tight linear relationship between the concentration of microplankton chlorophyll a and total chlorophyll a ($r^2 = 0.993$, Po 0.001, $n = 29.5$), and microplankton chlorophyll a forms >95% of total chlorophyll a when the latter exceeds ~5 mg m^{-3}. This relationship emphasises that comparisons between seasons or different oceanographic areas on the basis of the relative proportions of different size fractions can be misleading; the normalisation involved means that an increase in one size fraction is inevitably associated with an apparent decrease in another, even when none is involved. A clear picture of the dynamics comes only from the comparison of absolute chlorophyll concentrations in the different size fractions (as in Fig. 13). Furthermore, the ecological consequences are easier to interpret: for example the feeding response of pelagic or benthic grazers is dictated by the absolute concentration of cells in a particular size-range, not the relative concentration.

At the RaTS site the intense summer bloom of large cells and colonial forms is superimposed upon a less intense bloom of nanophytoplankton (Fig. 12). Although the large cells are likely to dominate the flux to the benthos, for many smaller grazers it is the nanoflagellate bloom that provides the key food resource. This whilst the summer bloom in Antarctic waters is typically dominated by diatoms and the larger colonial phytoplankton, in winter it is the nanoplankton fraction that dominates the total chlorophyll (Figs. 12 and 13). This pattern has important consequences for the ecology of suspension feeders, in particular that organisms selecting smaller cells experience a significantly longer feeding period than do those taking the large cells that dominate the summer bloom (Barnes and Clarke, 1994; Barnes, 1995).

4.2. Macronutrient dynamics

The development of the summer phytoplankton bloom depletes mixed-layer macronutrients, with utilisation of phosphate and nitrate following classical Redfield stoichiometry

(Fig. 16B). Summer macronutrient levels offshore in northern Marguerite Bay exhibit a similar stoichiometry, with the slope of N:P covariation plots indicating utilisation rations of 13.9 (95% CL 13.5–14.4) in 2003 and 13.6 (13.0–14.2) in 2002 (data from Palmer-LTER programme, for January). These are estimates of utilisation based on covariation in nutrient concentrations, either from a single location over time (the RaTS data) or spatially extensive in a limited time frame (the Palmer LTER data). Using such data to estimate stoichiometric utilisation ratios assumes that primary production is the only process removing nutrients from the water column being sampled.

An alternative approach is to calculate the actual seasonal utilisation from the seasonal minimum and the previous winter maximum. For most oceanographic cruises this is not possible and so the nutrient deficit is estimated by comparing mixed-layer profiles with underlying water where nutrient concentrations are believed to be unaffected by production processes. Using this technique Serebrennikova and Fanning (2004) estimated N:P utilisation ratios in Marguerite Bay during the GLOBEC studies of 12.47 1.6 in 2001 and 11.17 1.3 in 2002. Although the RaTS data provide a seasonal picture for the mixed layer in Ryder Bay, sampling frequency has been sufficient to determine seasonal maximum and minimum values only since 2004. These data suggest N:P utilisation stoichiometry of 14.1 in 2004 and 9.6 in 2005.

The quasi-conservative tracer N^* is typically used to determine the extent to which oxidation of ammonium to nitrate, or reduction of nitrate to gaseous nitrogen, decouples the stoichiometry of N and P. The seasonal variation in N^* at the RaTS site (Fig. 16B) is driven principally by variation in P, and the seasonal plot of N:P ratio shows a very similar pattern to that of N^*. The low values of N^* in winter, especially June to November (Fig. 16B), coincide with the period when ammonium concentration is declining rapidly (Fig. 15A), suggesting that ammonium oxidation may be decoupling N and P dynamics to some extent, though the stoichiometry for the RatS data overall is close to Redfield.

Ammonium is a highly labile macronutrient, typically exhibiting marked variability over quite short temporal and spatial scales. Ammonium is recycled rapidly within the mixed layer, with an important source of regenerated (reduced) nitrogen being zooplankton and microbial metabolism. Ammonium dynamics are thus dominated by processes operating on a faster timescale than the predominantly seasonal dynamics of nitrate, phosphate and silicate. The lability of ammonium means that a complete picture of its dynamics requires knowledge of the complete water-column inventory (Serebrennikova and Fanning, 2004). Although logistic constraints present determination of regular water-column profiles at the RaTS station, a clear seasonal picture for ammonium dynamics at 15 m does emerge from the climatology (Fig. 15A). Maximum values occur in early winter (April and May), with a steady utilisation thereafter, through winter, reaching a minimum in spring (October and November), when ammonium can often be undetectable. This pattern indicates continuous utilisation by autotrophs over winter, at rates exceeding regeneration processes. These autotrophs may include Crenarchaea, which are known to be an important component of the microbial plankton in Antarctic waters (Murray et al., 1999; DeLong et al., 2002; Church et al., 2003). Ammonium levels then rise in summer when zooplankton and microbial metabolism provides regenerated nitrogen.

Silicate values are highly variable, and Si:N stoichiometrics correspondingly imprecise. For Ryder Bay the overall Si:N utilisation stoichiometry from the covariation plot is 1.67 (95% CL 1.12–3.23). The mean value is only slightly >1, suggesting no significant limitation by Fe or other micronutrients, and none would be expected in a coastal location such as Marguerite Bay. Calculations based on seasonal depletion data are slightly higher: 2.38 for 2004 and 2.34 for 2005, and estimates for northern Marguerite Bay from GLOBEC data were 3.97 1.2 for 2001 and 4.17 1.1 in 2002 (Serebrennikova and Fanning, 2004). These values are broadly in agreement (given the imprecision involved and the differences in calculation), but noticeably higher than the overall mean value for the RaTS data.

The RaTS station in Ryder Bay is in the lee of Adelaide Island. Whilst the coastal location allows year-round sampling, it is also towards one extreme of the gradients of physics and biology that characterise the continental shelf of the western Antarctic Peninsula. In particular the influence of glacial meltwater increases towards the coast (Dierssen et al., 2002), and phytoplankton blooms together with the associated nutrient depletion also tend to be stronger nearer the coast (Garibotti et al., 2003; Serebrennikova and Fanning, 2004; Martinson et al., 2008). The input of heat and nutrients from flooding of UCDW across the shelf will tend to decrease with distance from the shelf-break, though the dynamics are heavily influenced by bathymetry (Dinniman and Klinck, 2004). Penetration of UCDW is detectable at the RaTS site, and across the WAP area every year (Ducklow et al., 2007), and this is critical to the nutrient balance in Marguerite Bay.

4.3. Comparison with Signy Island

The waters over the continental shelf to the west of the Antarctic Peninsula exhibit a clear latitudinal cline in many environmental features. From an ecological perspective, the most important of these are photoperiod, temperature and ice dynamics. Surface temperature in January shows a distinct variation north to south along the shelf (Fig. 1A, Martinson et al., 2008) and this variation is also evident in both mean temperature and seasonal range at shallow depths (Barnes et al., 2006).

Sea-ice dynamics also vary significantly, both along and across the WAP continental shelf. There are strong north to south, and across-shelf, gradients in the mean dates of ice advance, ice retreat and winter ice duration (Stammerjohn et al., 2008). Furthermore, all of these are showing strong secular changes associated with regional climate change (Stammerjohn et al., 2008); this is in marked contrast to the rest of Antarctica where sea-ice dynamics typically show no statistically significant long-term change (Kwok and Comiso, 2002). A notable exception is western Ross Sea, which shows a significant positive trend in sea ice (Stammerjohn et al., 2008).

These latitudinal trends mean that it would be valuable to compare the seasonal cycle at Rothera with other sites along the WAP. The only site in Antarctica for which similar long-term and year-round data exist is Signy Island (Clarke et al., 1988; Clarke and Leakey, 1996). Although Signy Island lies to the north of the Antarctic Peninsula, its oceanographic setting in the Atlantic basin and on the western edge of the Weddell gyre mean that comparison with data from the RaTS station needs to be undertaken with care. In addition the data at Signy Island come from a very shallow site (15 m in a water depth of $\sim$30 m) where mixed-layer processes are influenced by a strong glacial input and direct interaction with the seabed.

The long-term average seasonal cycle of temperature at 15 m is similar at Signy and the RaTS station (Fig. 17A). Minimum temperatures in winter are usually close to the freezing point of seawater, and maximum temperatures are reached in summer, typically in late January or early February. Although the average summer peak temperatures at the two sites are similar, temperature rises about 2 weeks later at the RaTS station, and falls about 1 week earlier. In consequence the thermal environment

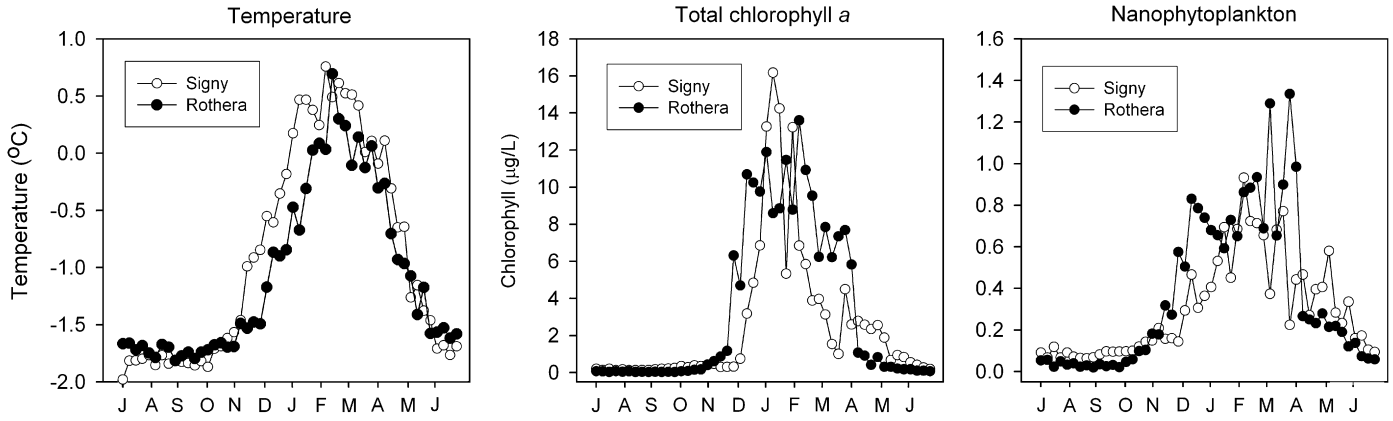

Fig. 17. A comparison of long-term mean data for Signy and Rothera. All data are for 15 m depth. Signy data are for 1988–1994, Rothera data are for 1997–2005; all data pooled by week: (A) temperature, (B) total chlorophyll *a* and (C) nanoplankton chlorophyll *a*. Note that data re plotted from midwinter (July) to midwinter (June) so that the austral summer season lies in the centre of the plot.

encountered by organisms living at the two sites differ. The mean number of degree-days integrated above an arbitrary threshold of −1.5 1C is thus 262 for Signy (averaged 1989–1994) but only 187 (averaged 1998–2005) for the RaTS station. Since all physiological processes are influenced by temperature, this would indicate that in the absence of evolutionary or physiological compensation, and all other things (such as food availability) being equal, ecologically important processes such as growth, maturation of reproductive tissue or embryonic development will be more constrained seasonally at Ryder Bay than at Signy. In terms of temperature, the summer season in the mixed layer at Ryder Bay is thus later and shorter than at Signy Island.

In contrast, and perhaps surprisingly, the length of the water-column phytoplankton bloom is greater further south at the RaTS station compared with Signy (Fig. 17B). Winter levels of total chlorophyll *a* (averaged over all years and pooled for July–September) are lower at Rothera (0.051 mg m^{-3}, SE 0.006, $n = 54$) than at Signy (0.190 mg m^{-3}, SE 0.014, $n = 58$), but mean summer peak values are slightly greater at Signy. The bloom dynamics are different at the two sites, with the initial rapid rise in spring chlorophyll concentrations occurring about 2 weeks earlier in Ryder Bay. This earlier start is presumably related to the different photoperiod and ice dynamics at the two sites, and deep mixing at Ryder Bay.

Although the seasonal variation in total chlorophyll *a* is driven principally by microplankton, many grazers utilise the nanoplankton fraction. Barnes (1995) has shown how the annual growth performance of the erect bryozoan *Cellarinella watersi* at Signy is related to the length of the annual nanophytoplankton bloom. Comparison of the two sites indicates that on average the nanoplankton bloom starts earlier and dies away later in Ryder Bay compared with Signy. Winter nanoplankton chlorophyll levels are lower at Ryder Bay (0.020 mg m^{-3}, SE 0.002, $n = 54$) than at Signy (0.086 mg m^{-3}, SE 0.005, $n = 63$), and there is no indication at Ryder Bay of the secondary autumn nanophytoplankton bloom observed at Signy (Fig. 17C).

4.4. Comparison with other studies: the measurement of chlorophyll in nearshore antarctic waters

Chlorophyll *a* is estimated by oceanographers with a wide range of techniques, and it is not always straightforward to achieve agreement between them. For the RaTS programme chlorophyll *a* is extracted into chloroform-methanol, which is believed to achieve a more complete extraction of photosynthetic pigments than the acetone used traditionally by oceanographers (Wood, 1985). Cross-calibration with acetone extraction indicated that the results from the two techniques are tightly correlated (Fig. 3C) and hence interconversion between the two methods is straightforward and precise. For a large bloom of 20 mg m^{-3} chlorophyll *a*, acetone extracts 54% of the pigment extracted by chloroform-methanol, and for a small bloom of 1 mg m^{-3} the value is 46%. These are very similar to the values reported originally by Wood (1985), which had a median value of 59% for a range of pure cultures of chlorophytes, chrysophytes and cyanophytes.

Phytoplankton comprises a complex assemblage of photoautotrophs, containing a wide range of pigments (Quigg et al., 2003), and it has long been recognised that this chemical complexity affects the accuracy and precision of bulk assays by spectrophotometry or fluorometry. Generally the ratio of fluorescence before and after acidification fell within the bounds expected for samples dominated by chlorophyll *a*, but in summer occasional samples some samples showed characteristics of interference from other fluorescent compounds in the extract. Multi-wavelength spectroscopy (Richards and Thompson, 1952; Jeffrey and Humphrey, 1975) confirmed this, suggesting the presence of significant amounts of chlorophyll *b* from cryptophytes.

The advent of ocean-colour sensors on satellites has revolutionised our understanding of the distribution and dynamics of phytoplankton in the global ocean (Longhurst, 1998). Optical observations in polar regions have proved particularly challenging because of low sun angles, long atmospheric path lengths, frequent cloudiness and interference from snow and ice (Dierssen and Smith, 2000). The algorithms for the conversion of optical reflectance data to an estimated chlorophyll concentration are also affected by the presence of scattering particles in the water, and a detailed study by Dierssen and Smith (2000) showed that the general processing algorithms for both the Coastal Zone Colour Scanner (CZCS) and Sea-viewing Wide Field-of-View Sensor (SeaWiFS) underestimated the chlorophyll content of oceanic waters along the WAP by a factor of ~2. This result was obtained for open-ocean waters where interference from inorganic particles in the water column is negligible. The RaTS station is relatively close to shore, and here the presence of glacial run-off can cause the seawater optical properties to be decoupled from chlorophyll concentration.

Examination of the PAR data taken at the RaTS station suggests that the optical depth of the water, defined as the depth at which PAR has decreased to 37% of the surface value, is above much of

the chlorophyll bloom in summer. Typical values for optical depth in December to March are ~5 m, during which period most of the chlorophyll lies in the range 10–40 m. Taken together, these three factors (glacial run off, proximity to ice, shallow optical depth) suggest that the value of remotely sensed reflectance data for estimating nearshore chlorophyll concentrations will be limited. Extractive techniques and observations *in situ* will continue to be essential for understanding the biological oceanography and ecology of the nearshore Antarctic marine system.

4.5. Interannual variability

Data obtained from observations at the RaTS station since 1997 have allowed us to define clearly the seasonal cycle in Ryder Bay, and we believe this is representative of conditions in northern Marguerite Bay. These data also have demonstrated the marked interannual variability characteristic of the Antarctic oceanic ecosystem. This interannual variability is evident in every variable measured, and is of powerful ecological importance. It is now clear that variability on interannual to subdecadal timescales, related to the El Niño Southern Oscillation and the Southern Annular Mode, is especially important in the Southern Ocean (Murphy et al., 1995; White and Peterson, 1996; Hall and Visbeck, 2002; Ducklow et al., 2007).

In some winters fast-ice forms and then stays in place for a long period (for example in 1997, 2000, 2002, 2003 and 2006). In others the presence of fast-ice is intermittent, sometimes forming and blowing out several times (for example 1998, 1999, 2001 and 2004). The very deep winter mixing observed in 1998 and 2003 were both associated with the decay of El Niño events. Although the duration of the RaTS programme to date is insufficient to detect statistically significant variability on subdecadal timescales, these observations point clearly to El Niño variability as an important driver for variability in mixed-layer processes, and the ecology that these influence in turn, in Ryder Bay (and, by extension, in Marguerite Bay).

Although the coldest temperatures at 15 m tend to be recorded in winters with long periods of fast-ice, there is no significant correlation between ice duration and mean winter mixed-layer temperature at 15 m in the data overall ($F = 1.02$; $P > 0.35$, $n = 9$). There is also significant interannual variability in the winter levels of both microplankton (>20 μm) and the larger nanoplankton (o 20–5 μm) chlorophyll *a* (Table 2). In both there is a trend for increasing values from 1997 to 2000, followed by lower levels thereafter (Table 2). The concentration of chlorophyll *a* in the two size fractions was strongly correlated (Pearson $r = 0.79$, $P = 0.034$, $n = 7$), and nanoplankton chlorophyll *a* exceeded that in the microplankton fraction by a factor of 4.3–1.1 (Table 2).

Table 2
Interannual variability in winter conditions, Ryder Bay, northern Marguerite Bay

Year	Ice (days)	Temp (1C)		Chlorophyll (mg m^{-3})		
		Mean	*n*	Mean (>20 μm)	Mean (o 20–5 μm)	*n*
1997	208	−1.813	11	0.007	0.030	12
1998	42	−1.728	8	0.008	0.026	10
1999	61	−1.691	3	0.015	0.036	3
2000	158	−1.690	2	0.038	0.043	2
2001	37	−1.629	3	*	*	0
2002	207	−1.650	12	0.002	0.005	13
2003	61	−1.735	8	0.006	0.014	9
2004	102	−1.736	5	0.007	0.011	5
2005	200	−1.764	7	*	*	*
2006	*	*	*	*	*	*

Ice is the total number of days with complete fast ice coverage, summed over all periods within that winter (intervening periods of open water or partial ice cover, should they occur, are not included in the total). Temperature and chlorophyll data are for 15 m depth at the RaTS station, averaged over the winter period (1 July–30 September); n is the number of winter observations in that year.

Table 3
Interannual variability in summer conditions, Ryder Bay, northern Marguerite Bay

Season	Temperature		Chlorophyll (>20 μm)		Chlorophyll (20–5 μm)	
	Start	K-days	Start	Dur	Start	Dur
1997/8	*	176	2	85	309	188
1998/9	315	266	322	99	276	220
1999/2000	305	137	282	205	281	249
2000/1	*	(276)	*	*	*	*
2001/2	*	(164)	*	*	*	*
2002/3	304	169	343	113	326	195
2003/4	325	275	293	191	286	226
2004/5	311	138	309	147	309	175
2005/6	*	*	*	*	*	*

All data are for 15 m depth at the RaTS station. The temperature data are the date (Start: day number) that temperature first exceeds −1.5 1C, and the number of degree-days (K-days) integrated above an arbitrary threshold of −1.5 1C. The chlorophyll data show the date (Start: day number) that the microplankton (>20 μm) bloom first exceeds 0.05 mg m^{-3} and the total number of days (Dur) above this threshold, and similarly for nanoplankton (20–5 μm) above a threshold of 0.01 mg m^{-3}. Missing data (*) are for seasons when logistic constraints on sampling prevented determination of the date on which the threshold values were crossed. Integrated degree-days for the 2000/1 and 2001/2 summers can be estimated, and these less precise data are shown in parentheses.

Table 4
Correlation (Pearson *r*) of the timing of the start of microplankton (>20 μm) and nanoplankton (20–5 μm) blooms with environmental variables

	Pearson *r*	*P*	*n*
Microphytoplankton (bloom threshold 0.5 mg m^{-3})			
Ice out date	0.844	0.035	5
Critical depth date	0.729	0.162 NS	5
Temperature	−0.307	0.615 NS	5
Nanophytoplankton (bloom threshold 0.1 mg m^{-3})			
Ice out date	0.838	0.037	5
Critical depth date	0.381	0.527 NS	5
Temperature	−0.467	0.427 NS	5

Ice out date is the date on which fast-ice blew out. Critical depth date is the date on which the mixed layer depth was first exceeded by the depth of net photocompensation irradiance (NPI: 15 μE m^{-2} s^{-1}). Temperature is the date on which temperature first exceeded an arbitrary threshold of −1.5 1C. NS: not significant ($P > 0.05$).

Summer conditions also exhibit marked interannual variation. The date on which temperature at 15 m first exceeds an arbitrary threshold of −1.5 1C varied relatively little, from early to late November. In contrast the integrated thermal environment (number of degree-days above −1.5 1C) varied from 138 to 276, a factor of 2. Compared with data for Signy, the range of interannual variability is slightly less, and the integrated thermal environment slightly cooler. There was also marked variation in the timing and duration of both the microplankton and nanoplankton blooms (Table 3), with the start of the bloom being correlated significantly with the timing of ice break-out: a delay in the date of ice break-out leads to a later bloom (Table 4).

The critical depth theory of Sverdrup (1953) relates the development of the phytoplankton bloom to the timing of the seasonal shallowing of the mixed layer, and specifically when the depth of net photocompensation irradiance (taken here to be 15 μE m^{-2} s^{-1}) first exceeds the mixed-layer depth. The date when these two variables cross (the date of critical depth) is closely matched by the mean date at which the phytoplankton bloom exceeds 1 mg m^{-3}. However, the bloom starts much earlier than

this, and when examined on a year by year basis, the timing of the phytoplankton bloom is uncorrelated with the shallowing of the mixed layer above NPI depth (Table 4). Neither is the timing of the bloom related to the timing of the summer warming of the mixed layer (Table 4).

The data from the RaTS programme to date thus suggest that the key annual events influencing much of the biological oceanography of northern Marguerite Bay are the formation and break-out of winter fast-ice. Since the western Antarctic Peninsula is currently experiencing rapid regional climate change, manifested in a significant change in sea-ice dynamics (Stammerjohn and Smith, 1996, 1997; Stammerjohn et al., 2003; Stammerjohn et al., 2008) and increasing surface water temperature (Meredith and King, 2005), we can expect significant changes at many levels of the oceanic food-web (Clarke et al., 2007). Continuation of existing time-series data sets for the WAP area (RaTS, Palmer-LTER) will be important if we are to understand the impacts of regional climate change in this area.

Acknowledgements

Data collection for the RaTS programme is undertaken by overwintering Marine Assistants, without whose dedication and hard work, often in less than pleasant weather, the study would not be possible. It is a pleasure to acknowledge the contributions of Alice Chapman (winters of 1997, 1998), Jenny Beaumont (1999, 2000), Rayner Piper (2001, 2002), Andrew Miller (2003, 2004), Paul Mann (2005) and Helen Rossetti (2006). We also gratefully acknowledge the essential support to the RaTS programme provided by a series of Boating Officers and Field Diving Officers, as well as many other members of Rothera Research Station for their help with CTD casts and water sampling. The RaTS programme has benefited enormously from close ties with the Palmer-LTER programme, and we are especially grateful for the opportunity to undertake regular cross-calibration exercises on the US research vessel *Laurence M. Gould*. Data from the Palmer LTER data archive were supported by Office of Polar Programs, NSF Grants OPP-9011927, OPP-9632763 and OPP-0217282. Finally, we would like to thank Helen Peat for maintaining the RaTS database, Andrew Fleming for provision of remotely sensed data, Peter Fretwell for maps and GIS expertise, and S. Papadimitrio, P. Morris, D. Evans and V. Giannelli for help with the DOC analyses.

References

Anderson, L.A., Sarmiento, J.L., 1994. Redfield ratios of remineralisation determined by nutrient data analysis. Global Biogeochemical Cycles 8, 65–80.

Barnes, D.K.A., 1995. Seasonal and annual growth in erect species of Antarctic bryozoans. Journal of Experimental Marine Biology and Ecology 188, 181–198.

Barnes, D.K.A., Clarke, A., 1994. Seasonal variation in the feeding activity of four species of Antarctic bryozoan in relation to environmental factors. Journal of Experimental Marine Biology and Ecology 181, 117–131.

Barnes, D.K.A., Fuentes, V., Clarke, A., Schloss, I.R., Wallace, M.I., 2006. Spatial and temporal variation in shallow seawater temperatures around Antarctica. Deep-Sea Research, Part II 53, 853–865.

Barth, J.A., Cowles, T.J., Pierce, S.D., 2001. Mesoscale physical and bio-optical structure of the Antarctic Polar Front near 170°W during austral spring. Journal of Geophysical Research 106, 13879–13902.

Beardsley, R.C., Limeburner, R., Owens, W.B., 2004. Drifter measurements of surface currents near Marguerite Bay on the western Antarctic Peninsula shelf during austral summer and fall, 2001 and 2002. Deep-Sea Research, Part II 51, 1947–1964.

Boyd, P.W., Robinson, C., Savidge, G., Williams, P.J.l.B., 1995. Water column and sea-ice production during austral spring in the Bellingshausen Sea. Deep-Sea Research, Part II 42, 1177–1200.

Bunt, J.S., 1960. Introductory studies of hydrology and plankton at Mawson, June 1956 to February 1957. ANARE Reports, Series B 3 (ANARE Publication 56), 1–135.

Carlson, C.A., Hansell, D.A., 2003. The contribution of DOM to biogeochemistry in the Ross Sea. In: DiTullio, J., Dunbar, R. (Eds.), Biogeochemical Cycles in the Ross Sea. Antarctic Research Series, vol. 78. American Geophysical Union, Washington, DC, pp. 123–142.

Catalano, G., 1987. An improved method for the determination of ammonia in seawater. Marine Chemistry 20, 289–295.

Church, M.J., DeLong, E.F., Ducklow, H.W., Karner, M.B., Preston, C.M., Karl, D.M., 2003. Abundance and distribution of planktonic Archaea and Bacteria in the waters west of the Antarctic Peninsula. Limnology & Oceanography 48, 1893–1902.

Clarke, A., 1988. Seasonality in the Antarctic marine ecosystem. Comparative Biochemistry and Physiology B—Biochemistry and Molecular Biology 90, 461–473.

Clarke, A., Leakey, R.J.G., 1996. The seasonal cycle of phytoplankton, macronutrients, and the microbial community in a nearshore Antarctic marine ecosystem. Limnology & Oceanography 41, 1281–1294.

Clarke, A., Holmes, L.J., White, M.G., 1988. The annual cycle of temperature, chlorophyll and major nutrients at Signy Island, South Orkney Islands, 1969–1982. British Antarctic Survey Bulletin 80, 65–86.

Clarke, A., Murphy, E.J., Meredith, M.P., King, J.C., Peck, L.S., Barnes, D.K.A., Smith, R.C., 2007. Climate change and the marine ecosystem of the western Antarctic Peninsula. Philosophical Transactions of the Royal Society of London, Series B 362, 149–166.

Deacon, G., 1984. The Antarctic Circumpolar Ocean. Cambridge University Press, Cambridge.

DeLong, E.F., Wu, K.Y., Prézelin, B.B., Jovine, R.V.M., 2002. High abundance of Archaea in Antarctic marine picoplankton. Nature 371, 695–697.

Dierssen, H.M., Smith, R.C., 2000. Bio-optical properties and remote sensing ocean color algorithms for Antarctic peninsula waters. Journal of Geophysical Research 105, 26301–26312.

Dierssen, H.M., Smith, R.C., Vernet, M., 2002. Glacial meltwater dynamics in coastal waters west of the Antarctic Peninsula. Proceedings of the National Academy of Sciences of the United States of America 99, 1790–1795.

Dinniman, M.S., Klinck, J.M., 2004. A model study of circulation and cross-shelf exchange on the west Antarctic Peninsula continental shelf. Deep-Sea Research, Part II 51, 2003–2022.

Ducklow, H.W., Fraser, W., Karl, D.M., Quetin, L.B., Ross, R.M., Smith, R.C., Stammerjohn, S.E., Vernet, M., Daniels, R.M., 2006. Water column processes in the west Antarctic Peninsula and the Ross Sea: interannual variations and foodweb structure. Deep-Sea Research, Part II 53, 834–852.

Ducklow, H.W., Baker, K., Fraser, W.R., Martinson, D.G., Quetin, L.B., Ross, R.M., Smith, R.C., Stammerjohn, S., Vernet, M., 2007. Marine ecosystems: the west Antarctic Peninsula. Philosophical Transactions of the Royal Society of London, Series B 362, 67–94.

Garibotti, I.A., Vernet, M., Ferrario, M.E., Smith, R.C., Ross, R.M., Quetin, L.B., 2003. Phytoplankton spatial distribution patterns along the western Antarctic Peninsula (Southern Ocean). Marine Ecology Progress Series 261, 21–39.

Gruber, N., Sarmiento, J.L., 1997. Global patterns of marine nitrogen fixation and denitrification. Global Biogeochemical Cycles 11, 235–266.

Hall, A., Visbeck, M., 2002. Synchronous vaiability in the southern hemisphere atmosphere, sea ice, and ocean resulting from the annular mode. Journal of Climate 15, 3043–3057.

Hart, T.J., 1934. On the phytoplankton of the south-west Atlantic and the Bellingshausen Sea, 1929–1931. Discovery Reports 8, 1–286.

Hofmann, E.E., Klinck, J.M., 1998. Thermohaline variability of the waters overlying the west Antarctic Peninsula continental shelf. In: Jacobs, S.S., Weiss, R.F. (Eds.), Ocean, Ice and Atmosphere: Interactions at the Antarctic Continental Margin. American Geophysical Union, Washington, DC, pp. 67–81.

Hofmann, E.E., Klinck, J.M., Lascara, C.M., Smith, D.A., 1996. Water mass distribution and circulation west of the Antarctic Peninsula and including Bransfield Strait. In: Ross, R.M., Hofmann, E.E., Quetin, L.B. (Eds.), Foundations for Ecological Research West of the Antarctic Peninsula. Antarctic Research Series, vol. 70. American Geophysical Union, Washington, DC, pp. 61–80.

Holmes, R.M., Aminot, A., Kérouel, R., Hooker, B.A., Peterson, B.J., 1999. A simple and precise method for measuring ammonium in marine and freshwater ecosystems. Canadian Journal of Fisheries and Aquatic Sciences 56, 1801–1808.

Jeffrey, S.W., Hallegraeff, G.M., 1987. Chlorophyllase distribution in ten classes of phytoplankton: a problem for chlorophyll analyses. Marine Ecology Progress Series 35, 293–304.

Jeffrey, S.W., Humphrey, G.R., 1975. New spectrophotometric equations for determining chlorophylls *a*, *b*, c_1 and c_2 in higher plants, algae and natural phytoplankton. Biochemie und Physiologie der Pflanzen 167, 211–217.

Klinck, J.M., 1998. Heat and salt changes on the continental shelf west of the Antarctic Peninsula between January 1993 and January 1994. Journal of Geophysical Research—Oceans 103, 7617–7636.

Kopczyńska, E.E., 1981. Periodicity and composition of summer phytoplankton in Ezcurra Inlet, Admiralty Bay, King George Island, South Shetland Islands. Polish Polar Research 2, 55–70.

Korb, R.E., Whitehouse, M., 2004. Contrasting primary production regimes around South Georgia, Southern Ocean: large blooms versus high nutrient, low chlorophyll waters. Deep-Sea Research, Part I 51, 721–738.

Krebs, W.N., 1983. Ecology of neritic diatoms, Arthur Harbor, Antarctica. Micropaleontology 29, 267–297.

Kwok, R., Comiso, J.C., 2002. Spatial patterns of variability in Antarctic surface temperature: connections to the southern hemisphere annular mode and the Southern Oscillation. Geophysical Research Letters 107, Art 1705.

Littlepage, J.L., 1965. Oceanographic observations in McMurdo Sound, Antarctica. Antarctic Research Series 5, 1–37.

Longhurst, A., 1998. Ecological Geography of the Sea. Academic Press, San Diego.
Martinson, D.G., Stammerjohn, S.E., Iannuzzi, R.A., Smith, R.C., Vernet, M., 2008. Western Antarctic Peninsula physical oceanography and spatiotemporal variability. Deep-Sea Research, Part II, this issue [doi:10.1016/j.dsr2.2008.04.038].
Massom, R.A., Stammerjohn, S.E., Smith, R.C., Pook, M.J., Iannuzzi, R.A., Adams, N., Martinson, D.G., Vernet, M., Fraser, W.R., Quetin, L.B., Ross, R.M., Massom, Y., Krouse, H.R., 2006. Extreme anomalous atmospheric circulation in the west Antarctic Peninsula region in austral spring and summer 2001/02, and its profound impact on sea ice and biota. Journal of Climate 19, 3544–3571.
Meredith, M.P., King, J.C., 2005. Rapid climate change in the ocean west of the Antarctic Peninsula during the second half of the 20th century. Geophysical Research Letters 32, L19604.
Meredith, M.P., Renfrew, I.A., Clarke, A., King, J.C., Brandon, M.A., 2004. Impact of the 1997/98 ENSO on upper ocean characteristics in Marguerite Bay, western Antarctic Peninsula. Journal of Geophysical Research 109, C09013, 19pp.
Meredith, M.P., Murphy, E.J., Hawker, E.J., King, J.C., Wallace, M.I., 2008. On the interannual variability of ocean temperatures around South Georgia, Southern Ocean: forcing by E1 Nino/Southern Oscillation and the southern annular mode. Deep-Sea Research, Part II, this issue [doi:10.1016/j.dsr2.2008.05.020].
Mitchell, B.G., Holm-Hansen, O., 1991. Observations and modeling of the Antarctic phytoplankton crop in relation to mixing depth. Deep-Sea Research 38, 981–1007.
Moffat, C., Beardsley, R.C., Owens, B., van Lipzig, N.P.M., 2008. A first description of the Antarctic Peninsula Coastal Current (APCC). Deep-Sea Research, Part II, in press [doi:10.1016/j.dsr2.2007.10.003].
Moline, M.A., Claustre, H., Frazer, T.K., Schofield, O., Vernet, M., 2004. Alteration of the food web along the Antarctic Peninsula in response to a warming trend. Global Change Biology 10, 1973–1980.
Mosby, H., 1936. The waters of the Atlantic Antarctic Ocean. Scientific Results of the Norwegian Antarctic Expedition, 1927–1928 11, 1–131.
Murphy, E.J., Clarke, A., Symon, C., Priddle, J.H., 1995. Temporal variation in Antarctic Sea ice: analysis of a long-term fast-ice record from the South Orkney Islands. Deep-Sea Research, Part I 42, 1045–1062.
Murray, A.W., Wu, K.Y., Moyer, C.L., Karl, D.M., DeLong, E.F., 1999. Evidence for circumpolar distribution of planktonic Archaea in the Southern Ocean. Aquatic Microbial Ecology 18, 263–273.
Obata, A., Ishizaka, J., Endoh, M., 1996. Global verification of critical depth theory for phytoplankton bloom with climatological *in situ* temperature and satellite ocean color data. Journal of Geophysical Research 101, 20567–20667.
Qian, J., Mopper, K., 1996. Automated high performance, high temperature combustion total carbon analyzer. Analytical Chemistry 68, 3090–3097.
Quigg, A., Finkel, Z.V., Irwin, A.J., Rosenthal, Y., Ho, T.-Y., Reinfelder, J.R., Schofield, O., Morel, F.M.M., Falkowski, P.G., 2003. The evolutionary inheritance of elemental stoichiometry in marine phytoplankton. Nature 425, 291–294.
Richards, F.A., Thompson, T.F., 1952. The estimation and characterization of plankton populations by pigment analyses. II. A spectrophotometric method for the estimation of plankton pigments. Journal of Marine Research 11, 156–172.
Serebrennikova, Y.M., Fanning, K.A., 2004. Nutirents in the Southern Ocean GLOBEC region: variations, water circulation, and cycling. Deep-Sea Research, Part II 51, 1981–2002.
Smith, D.A., Klinck, J.M., 2002. Water properties on the west Antarctic Peninsula continental shelf: a model study of effects of surface fluxes and sea ice. Deep-Sea Research, Part II 49, 4863–4886.
Solorzano, L., 1969. Determination of ammonia in natural waters by the phenolhypochlorite method. Limnology & Oceanography 14, 799–801.
Stammerjohn, S.E., Martinson, D.G. Smith, R.C., Iannuzzi, R.A., 2008. Sea ice in the Western Antarctic Peninsula region: spatio-temporal variability from ecological and climate change perspectives. Deep-Sea Research, Part II, this issue [doi:10.1016/j.dsr2.2008.04.026].
Stammerjohn, S.E., Drinkwater, M.R., Smith, R.C., Liu, X., 2003. Ice-atmosphere interactions during sea-ice advance and retreat in the western Antarctic Peninsula. Journal of Geophysical Research 108, 3329.
Stammerjohn, S.E., Smith, R.C., 1996. Spatial and temporal variability of western Antarctic Peninsula Sea ice coverage. In: Ross, R.M., Hofmann, E.E., Quetin, L.B. (Eds.), Foundations for Ecological Research West of the Antarctic Peninsula. Antarctic Research Series, vol. 70. American Geophysical Union, Washington, DC, pp. 81–104.
Stammerjohn, S.E., Smith, R.C., 1997. Opposing Southern Ocean climate patterns as revealed by trends in regional sea ice coverage. Climatic Change 37, 617–639.
Strickland, J.D.H., Parsons, T.R., 1968. A Practical Manual of Seawater Analysis. Fisheries Research Board of Canada, Ottawa.
Sverdrup, H.U., 1953. On conditions for the vernal blooming of phytoplankton. Journal du Conseil 18, 287–295.
Thomas, D.N., Dieckmann, G.S., 2003. Sea Ice: An Introduction to its Physics, Chemistry, Biology and Geology. Blackwell Science, Oxford.
Thomas, D.N., Kattner, G., Engbrodt, R., Giannelli, V., Kennedy, H., Haas, C., Dieckmann, G.S., 2001. Dissolved organic matter in Antarctic Sea ice. Annals of Glaciology 33, 297–303.
Wallace, M.I., 2008. Ocean circulation, properties and variability in Marguerite Bay, West Antarctic Peninsula. PhD Thesis, Open University, 272pp.
Wedborg, M., Hoppema, M., Skoog, A., 1998. On the relationship between organic and inorganic carbon in the Weddell Sea. Journal of Marine Systems 17, 59–76.
White, W.B., Peterson, R.G., 1996. An Antarctic circumpolar wave in surface pressure, wind, temperature and sea-ice extent. Nature 380, 699–702.
Whitehouse, M.J., Priddle, J.H., Symon, C., 1996. Seasonal and annual change in seawater temperature, salinity, nutrient and chlorophyll *a* distribution around South Georgia, South Atlantic. Deep-Sea Research, Part I 43, 425–443.
Wood, L.W., 1985. Chloroform methanol extraction of chlorophyll *a*. Canadian Journal of Fisheries and Aquatic Sciences 42, 38–43.